

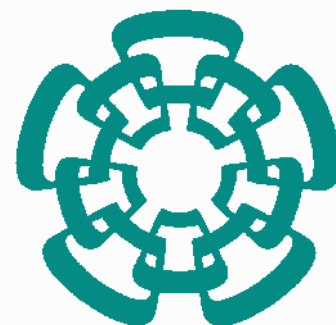
Magnetic Properties of Clusters from DFT Studies

J. Luis Torres-Moreno^a, Bernardo Zuniga-Gutierrez^b, Andreas M. Köster^a

^aDepartamento de Química, CINVESTAV
Av. Instituto Politécnico Nacional 2508
A.P. 14-740 México, D.F., C.P. 07360, México

^bDepartamento de Química,
Universidad de Guadalajara, CUCEI,
Blvd. Gral. Marcelino García Barragán 1421,
Olímpica, 44430 Guadalajara, Jalisco, México

Email: akoster@cinvestav.mx



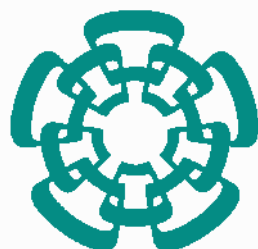
Clusters and Nanostructures Gordon Research Conference
Les Diablerets, Switzerland, June 2019

Outline

- Spin Magnetic Moments in Sodium Clusters
- Spin Magnetic Moments in V Doped Coin Metal Clusters
- ^1H NMR Shieldings in Polyhydrido Copper Cluster
- Conclusions

The deMon2k Community

<http://www.demon-software.com>



compute | calcul
canada



Electronic Shells in Simple Metal Clusters

deMon2k
density of Montréal

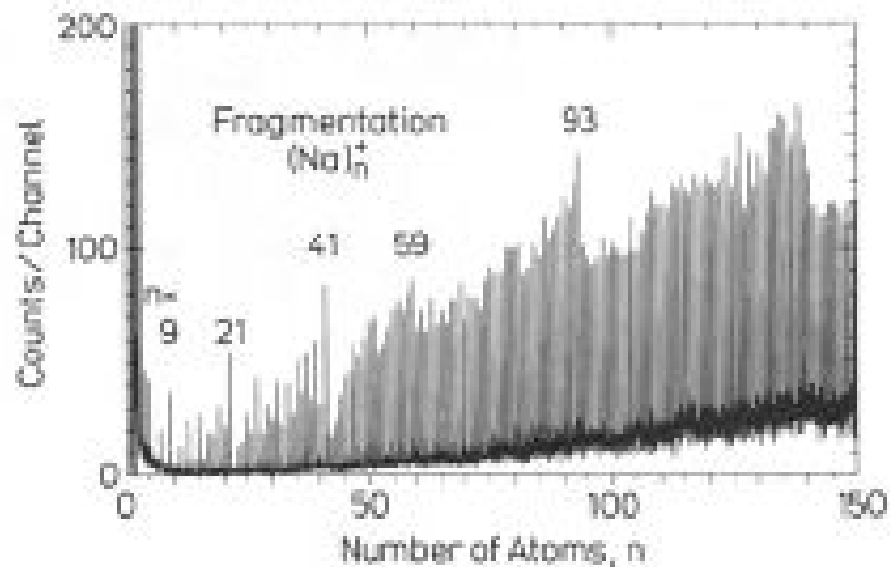
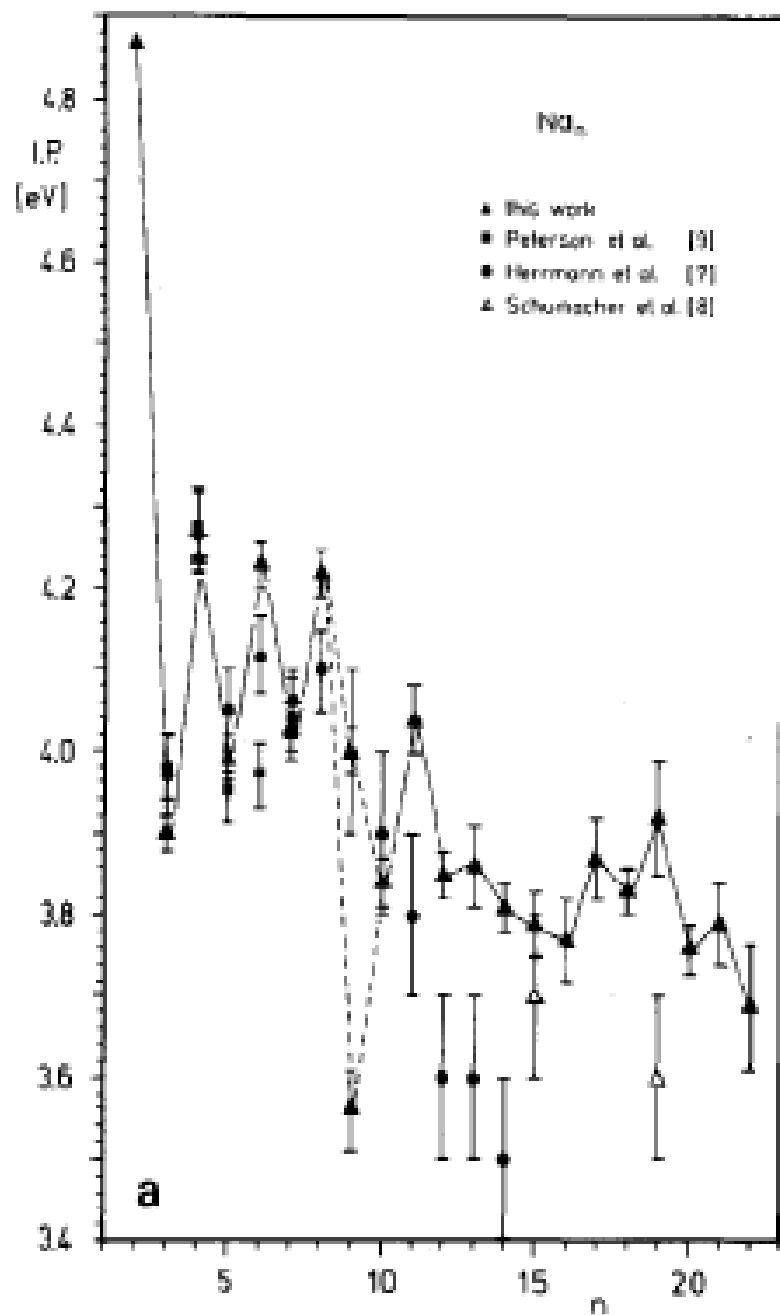
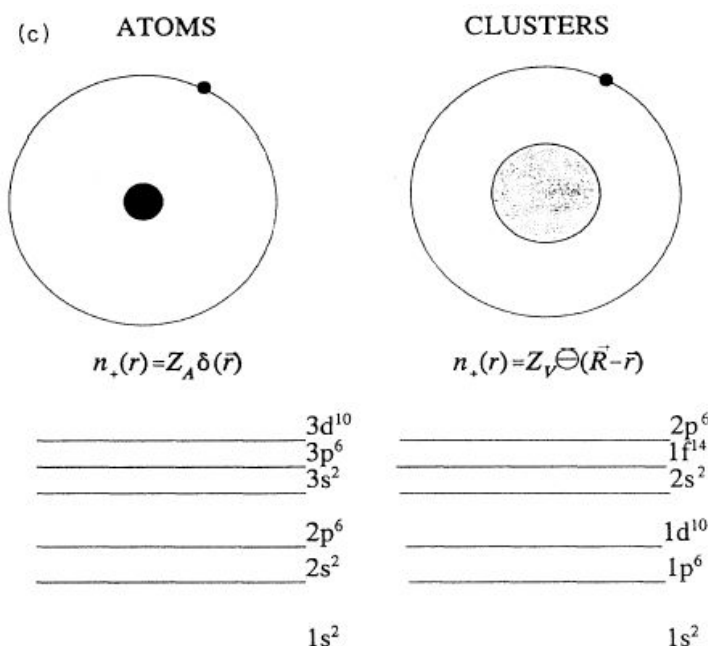


Figure 5. Mass spectrum of $(\text{Na})_n^+$ clusters ionized with high-intensity, 2.53-eV light. The clusters are fragmented by the ionizing laser. Fragments having closed-shell electronic configurations are particularly stable.

M.M. Kappes, M. Schär, U. Röthlisberger, C. Yeretzian, E. Schumacher, *Chem. Phys. Lett.* **143**, 251 (1988)

T.P. Martin, T. Bergmann, H. Göhlich, T. Lange, *J. Phys. Chem.* **95**, 6421 (1991)

Electronic Shells in Na_n Clusters



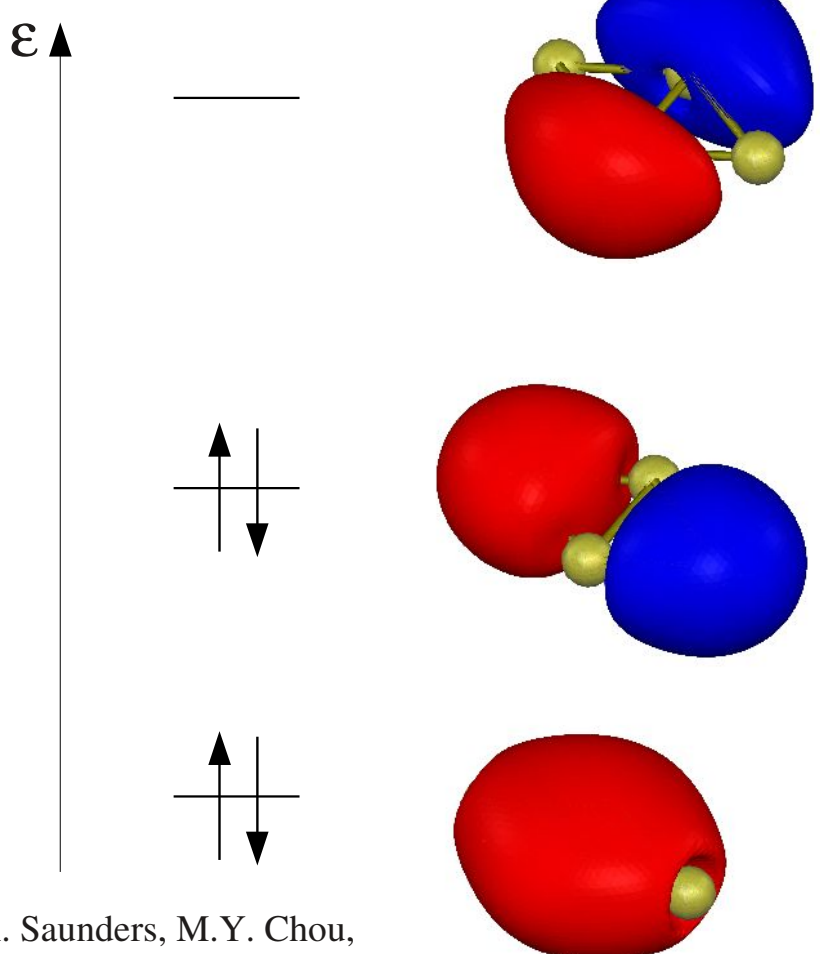
Na_9^+ (8e⁻): 1S² 1P⁶

Na_{21}^+ (20e⁻): 1S² 1P⁶ 1D¹⁰ 2S²

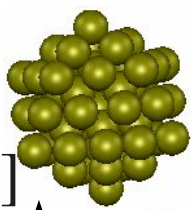
Na_{41}^+ (40e⁻): 1S² 1P⁶ 1D¹⁰ 2S² 1F¹⁴ 2P⁶

Na_{59}^+ (58e⁻): 1S² 1P⁶ 1D¹⁰ 2S² 1F¹⁴ 2P⁶ 1G¹⁸

MOs of Na_4 (4e⁻ \cong ³C) Cluster
Hund's rule \rightarrow JT distorsion

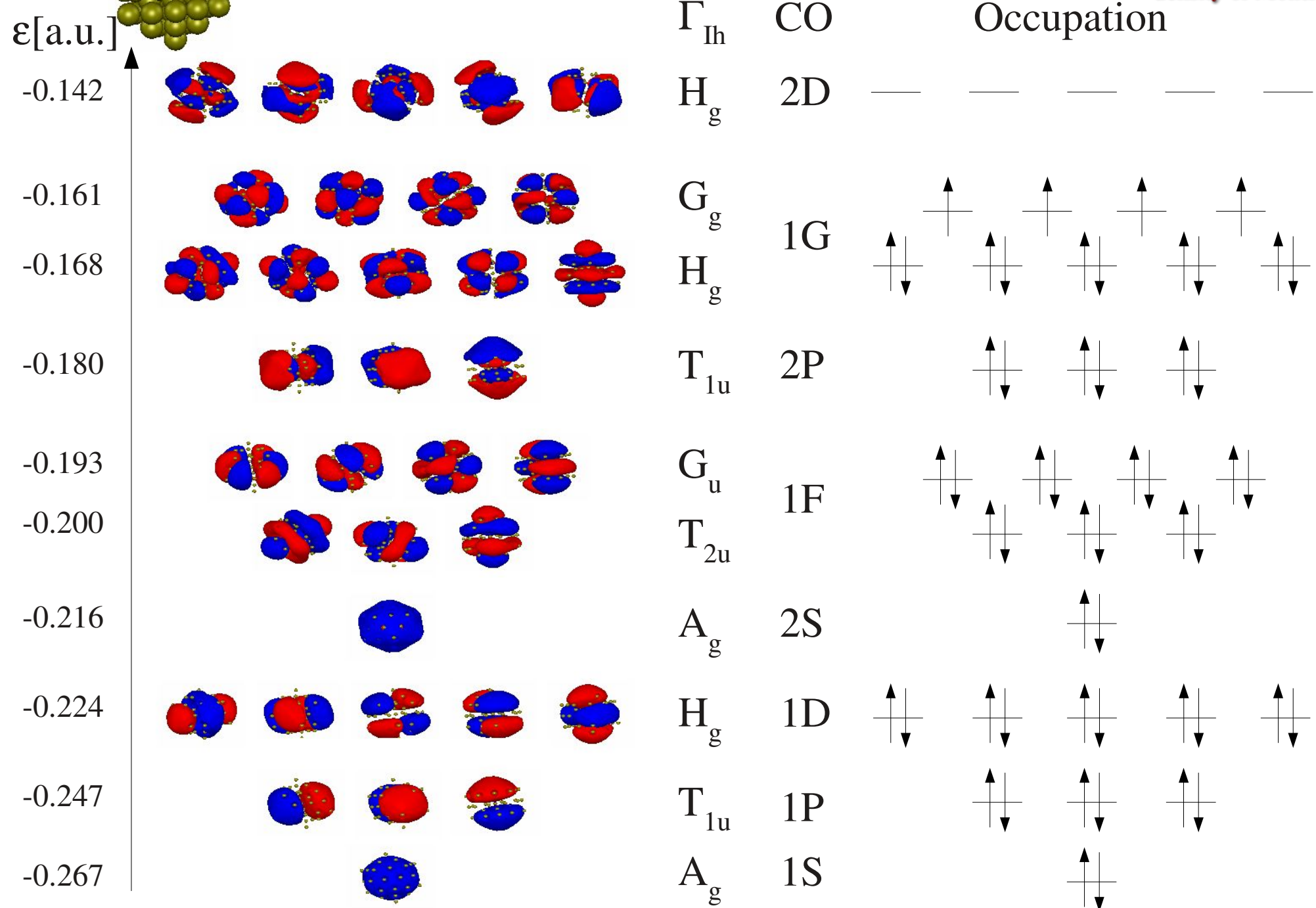


W.D. Knight, K. Clemenger, W.A. de Heer, W.A. Saunders, M.Y. Chou,
M.L. Cohen, *Phys. Rev. Lett.* **52**, 2141 (1984); S.N. Khanna, P. Jena, *Phys.
Rev. B* **51**, 13705 (1995); K. Jug, B. Zimmermann, A.M. Köster, *Int. J.
Quant. Chem.* **90**, 594 (2002)



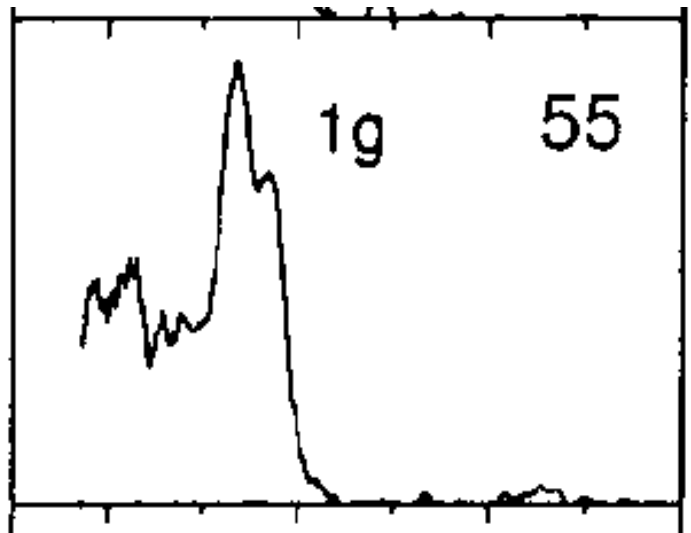
BUT: Molecular Orbital Analysis for Na_{55}^+

deMon2k
density of Montréal



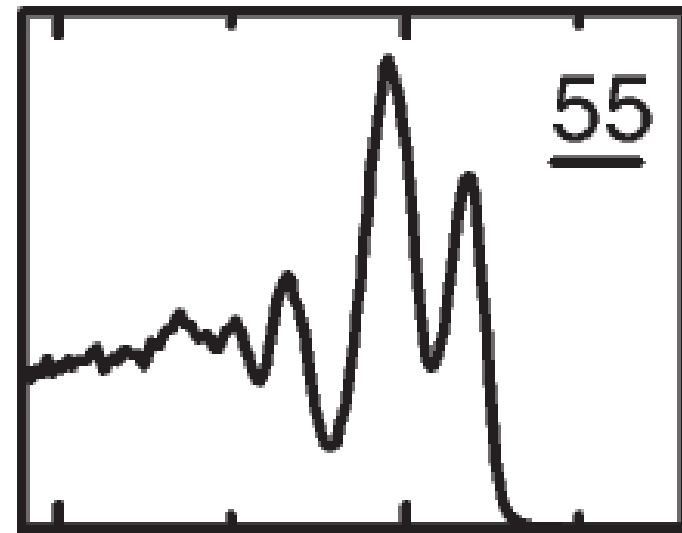
PES and DOS of Na_{55} Clusters

PES of Na_{55}^+



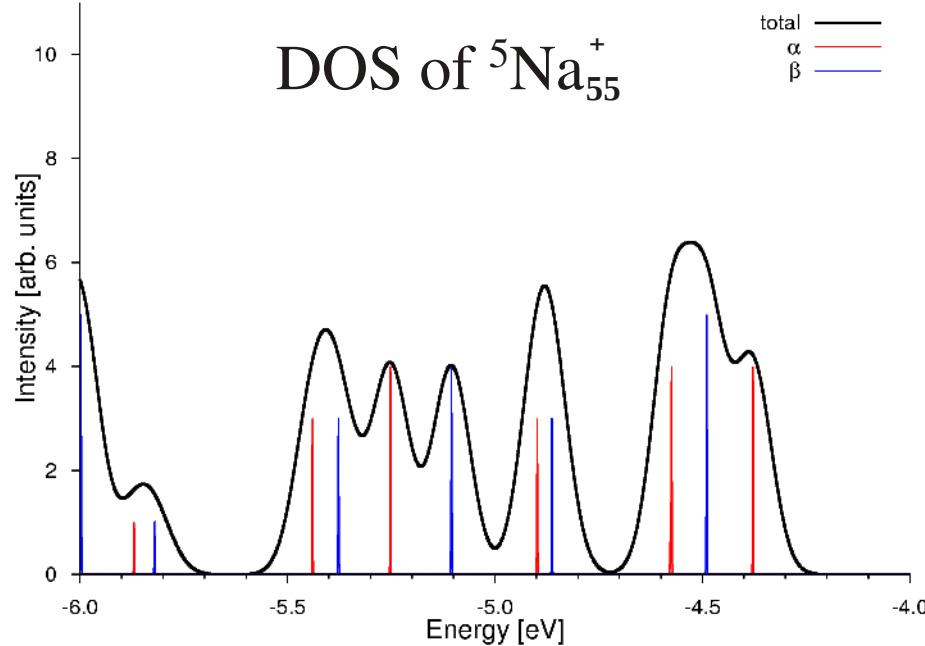
From: G. Wrigge et al. *Phys. Rev. A* **65**, 063201 (2002)

PES of Na_{55}^-

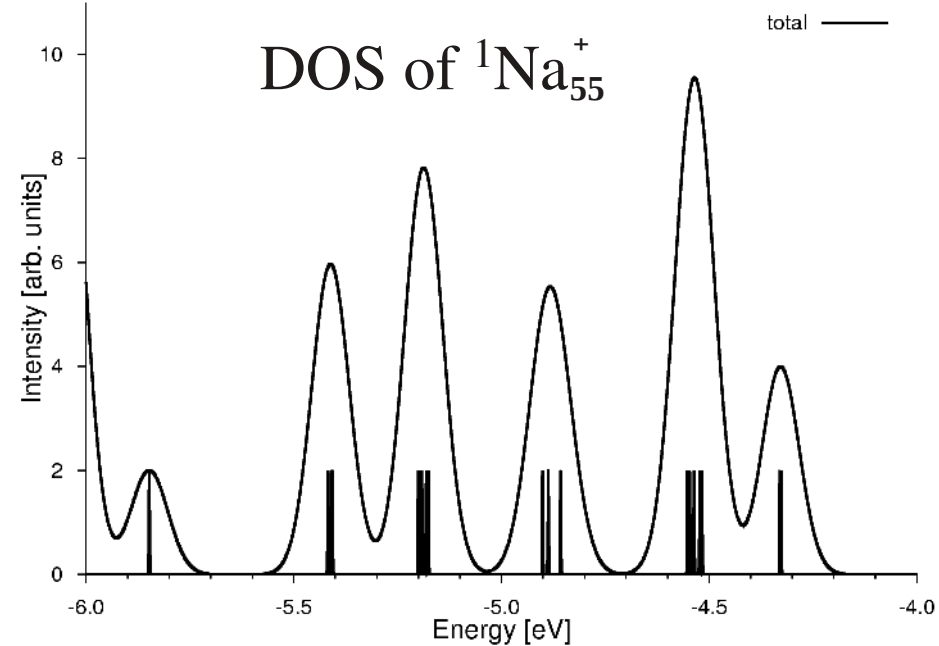


From: O. Kostko et al. *Phys. Rev. Lett.* **98**, 043401 (2007)

DOS of ${}^5\text{Na}_{55}^+$



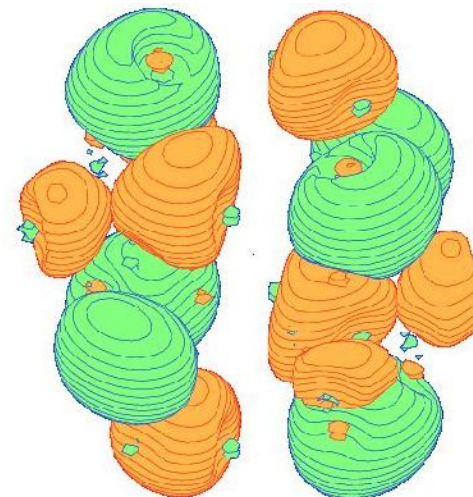
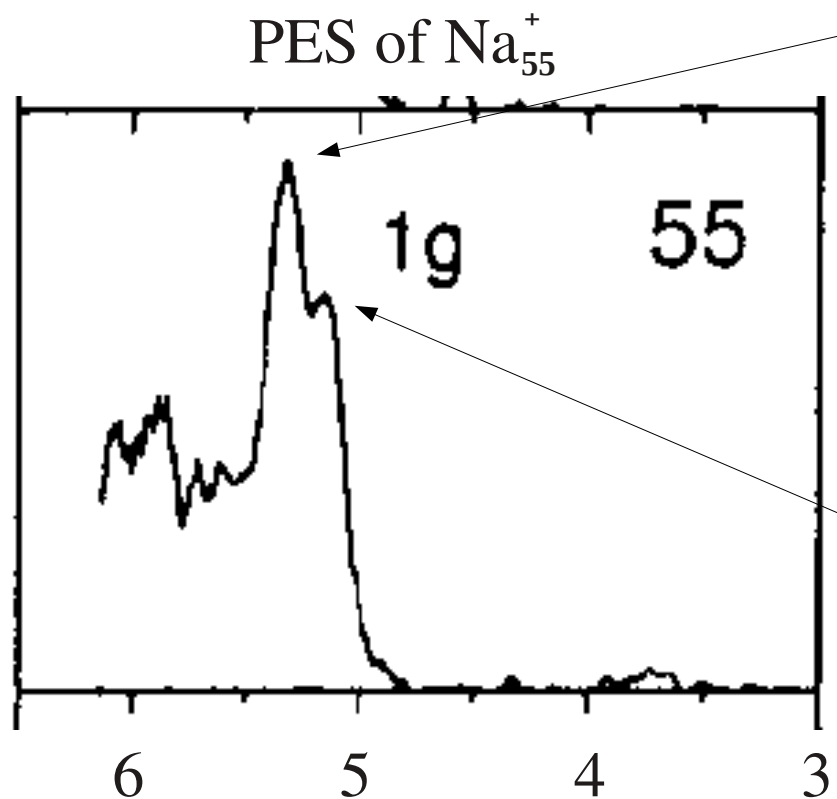
DOS of ${}^1\text{Na}_{55}^+$



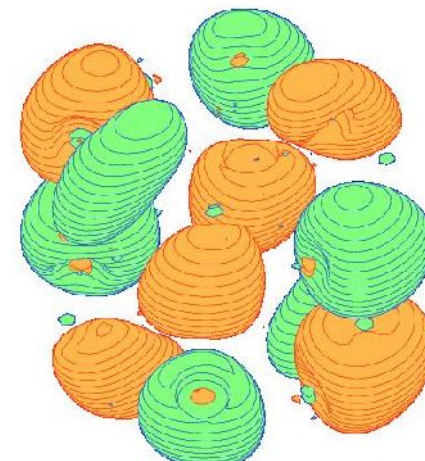
Propagator Calculations of ${}^5\text{Na}_{55}^+$ (V. Ortiz)

Method: P3+/6-311G(d)

Vertical electron detachment energies



${}^5\text{A}_{1g} - \text{e}^-$ from ${}^4\text{H}_g$ (5.66 eV)



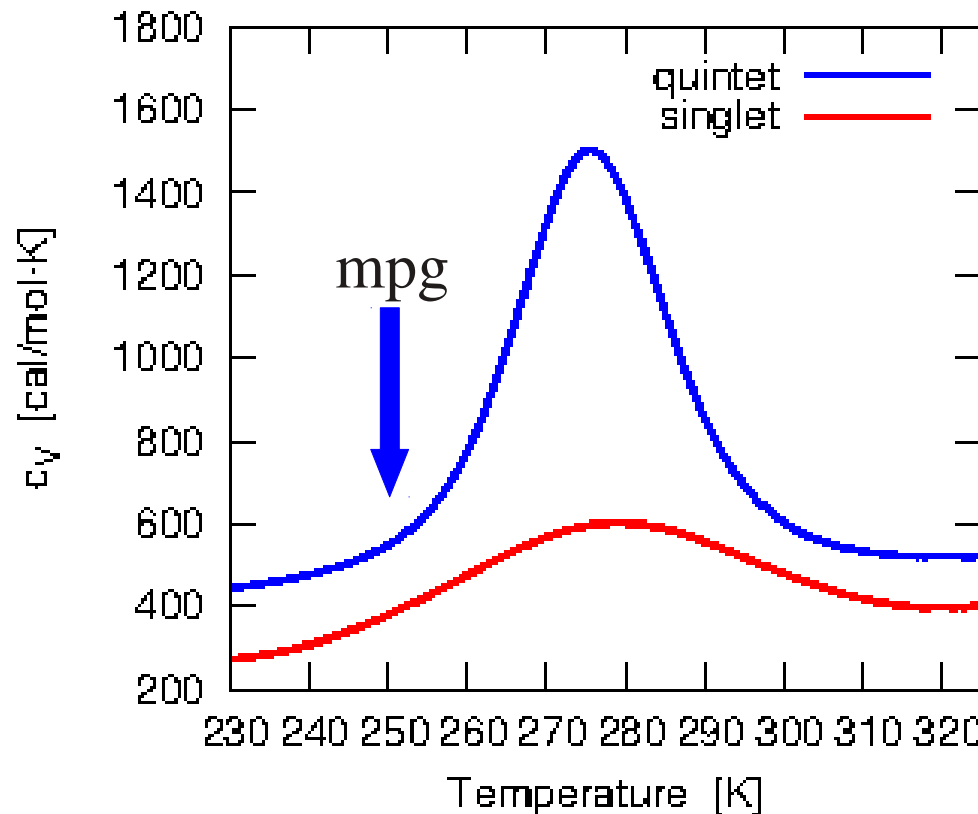
${}^5\text{A}_{1g} - \text{e}^-$ from ${}^4\text{G}_g$ (5.48 eV)

BOMD of ${}^5\text{Na}_{55}^+$

The LDA/GGA/Hybrid Na_{55}^+ ground state is a quintet in I_h symmetry.

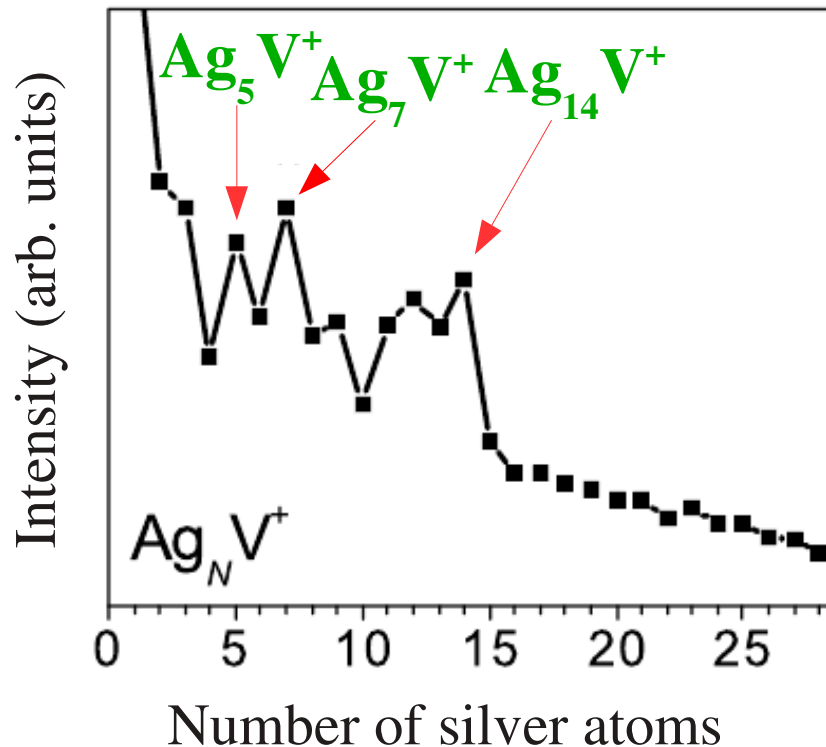
This gives rise to a relative large (~ 0.25 eV) HOMO-LUMO gap.

The HOMO is four-fold degenerated.



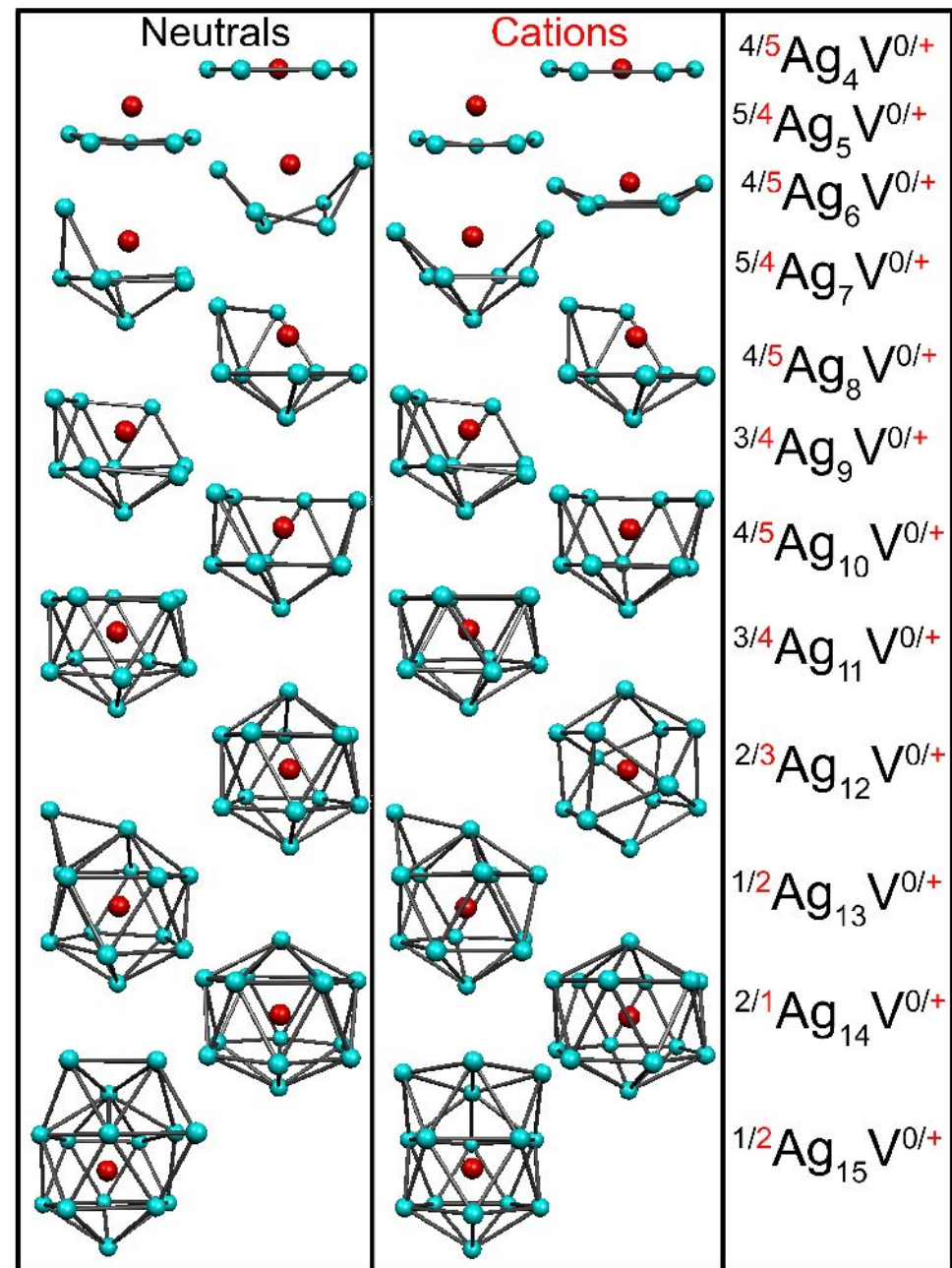
J.M. Vásquez-Pérez et al. *J. Phys. Chem. Lett.* **6**, 4646 (2015)

Mass Spectra & Optimized Structures of Ag_xV^+

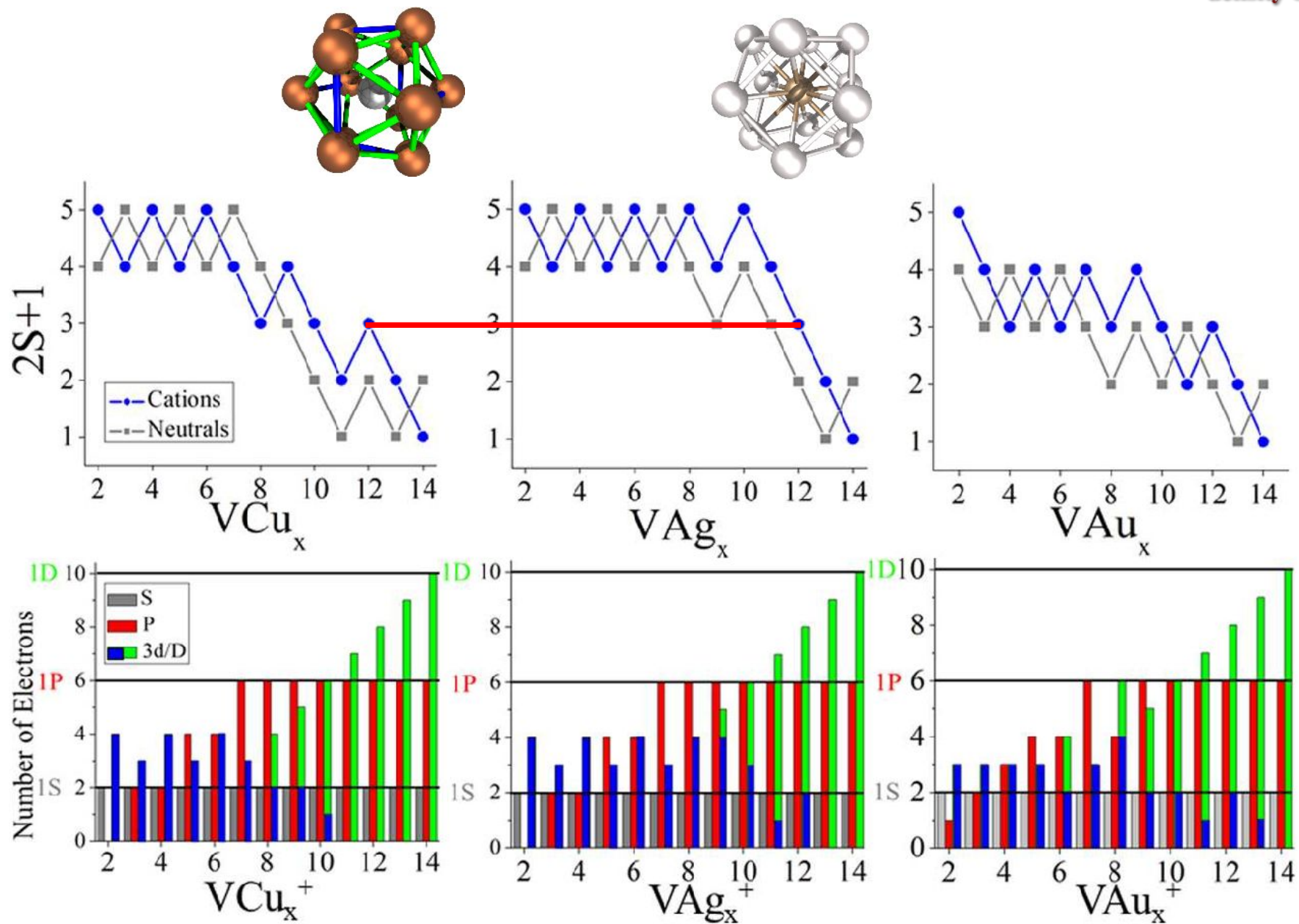


E. Janssens, S. Neukermans, H.M.T. Nguyen, M.T. Nguyen, P. Lievens, *Phys. Rev. Lett.* **94**, 113401 (2005)

V.M. Medel, A.C. Reber, V. Chauhan, P. Sen, A.M. Köster, P. Calaminici, S.N. Khanna, *J. Am. Chem. Soc.* **136**, 8229 (2014)



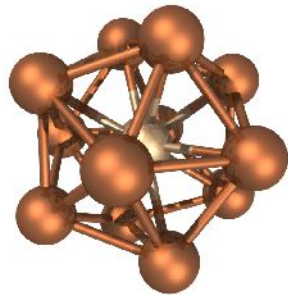
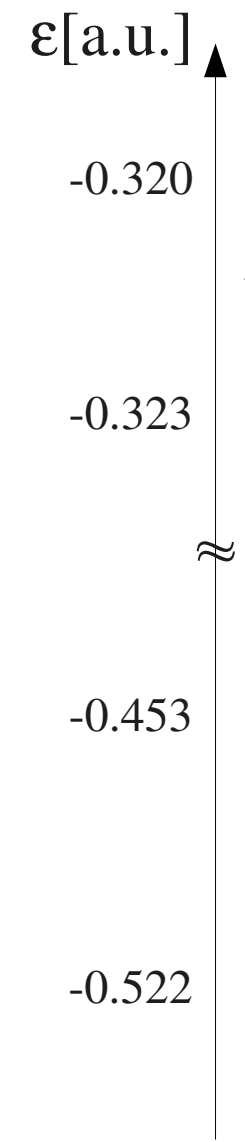
Electronic Structure of Cu_xV^+ , Ag_xV^+ and Au_xV^+



W.H. Blades, A.C. Reber, S.N. Khanna, L. Lopez-Sosa, P. Calaminici , A.M. Köster, *J. Phys. Chem. A* **121**, 2990 (2017)

MO Diagram of ${}^3\text{Cu}_{12}\text{V}^+$

deMon2k
density of Montréal



Γ_{Ih} CO

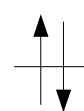
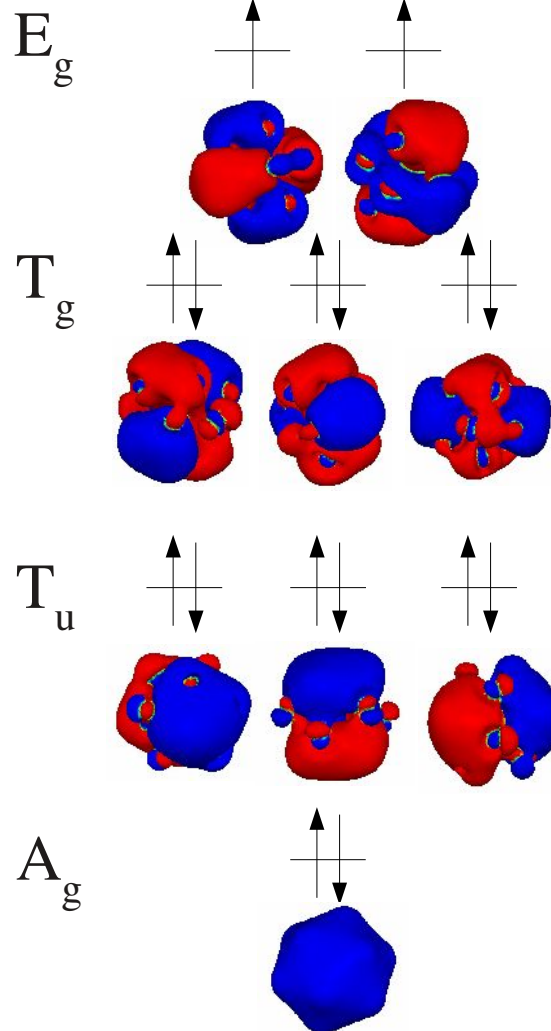
Γ_{Th}

d manifold

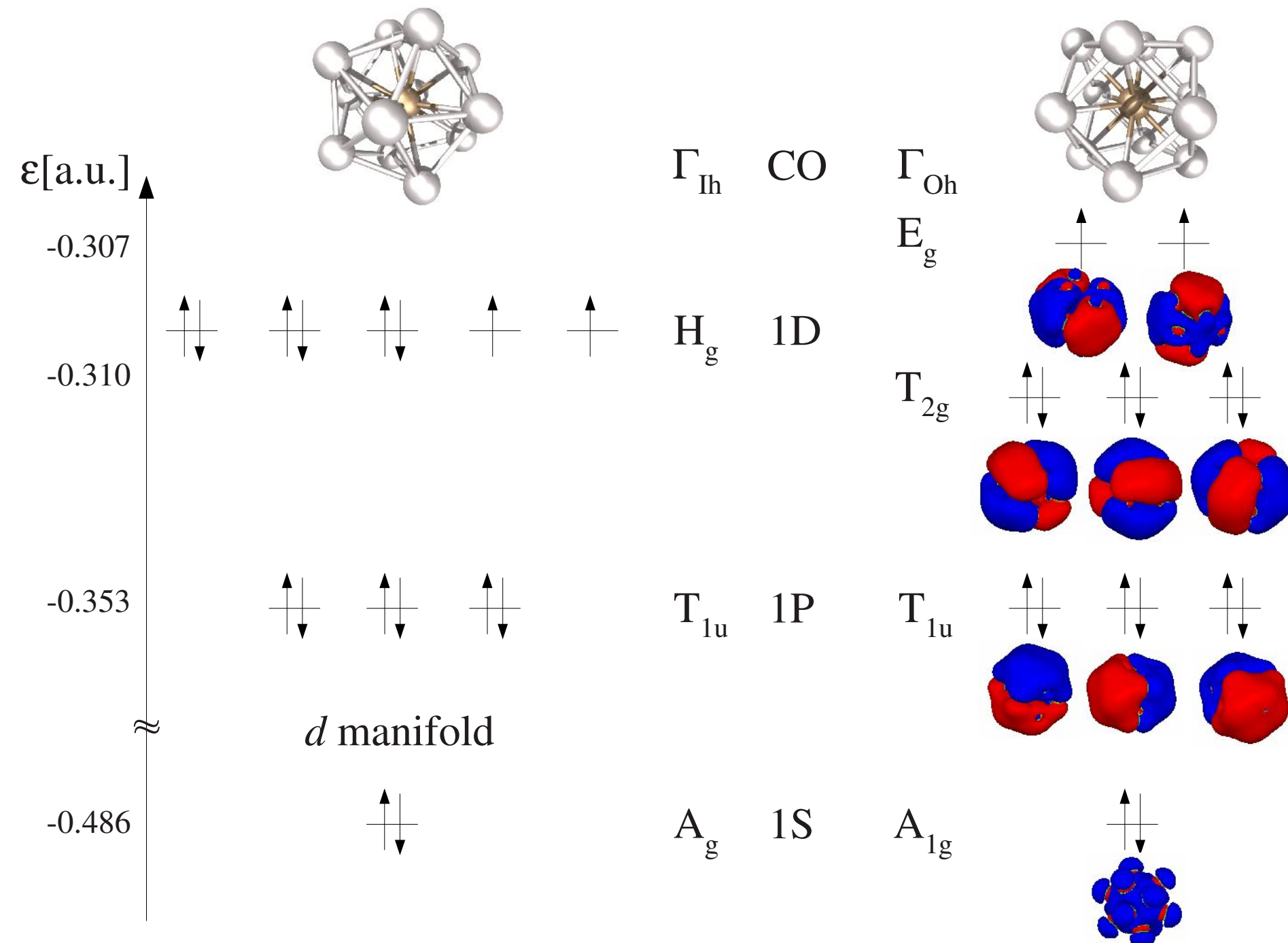
H_g 1D

$\text{T}_{1\text{u}}$ 1P

A_g 1S

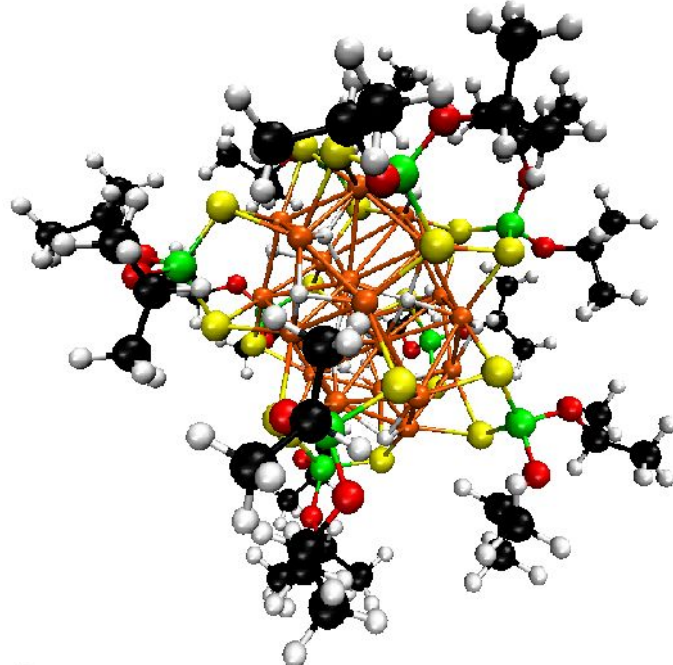


MO Diagram of ${}^3\text{Ag}_{12}\text{V}^+$

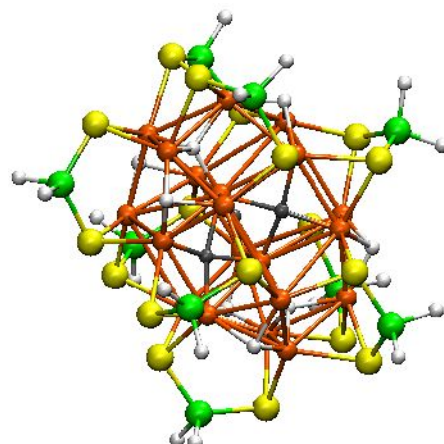
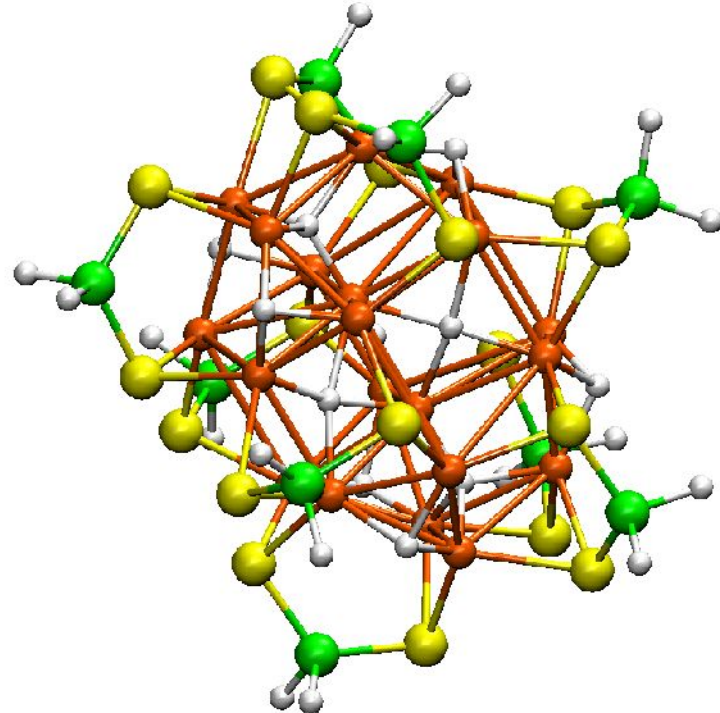


Polyhydrido Copper Cluster

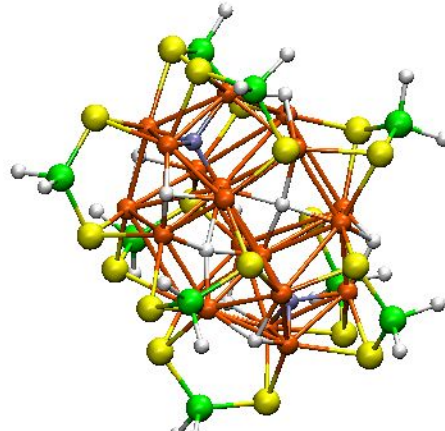
Experimental System $\text{Cu}_{20}\text{H}_{11}[\text{S}_2\text{P}(\text{O}^{\text{i}}\text{Pr})_2]_9$



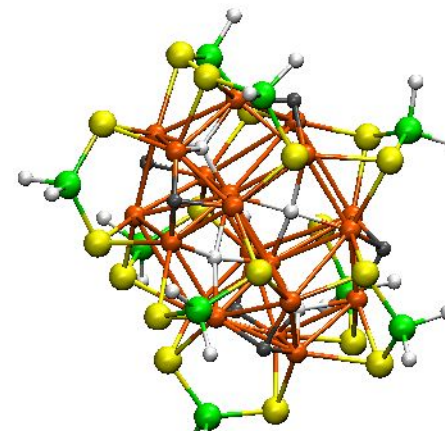
$\text{C}_{3\text{h}}$ Model System $\text{Cu}_{20}\text{H}_{11}[\text{S}_2\text{PH}_2]_9$



$\mu_4\text{-H}_{\text{square}}$



$\mu_4\text{-H}_{\text{tet}}$



$\mu_3\text{-H}$

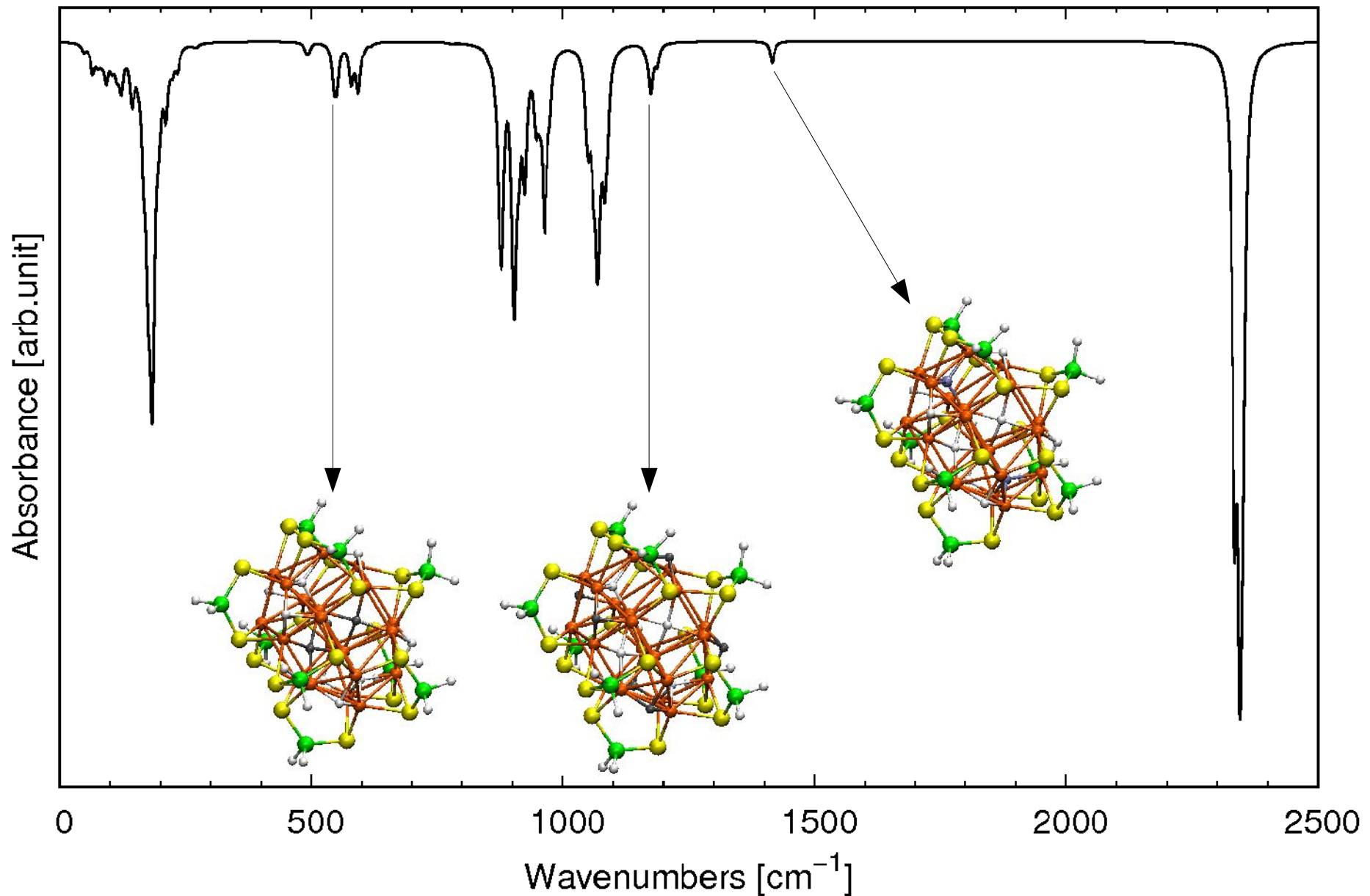
Optimized Cu-H Bond Lengths

Hydrogen	Cu-H [Å]
$\mu_4\text{-H}_{\text{square}}$	1.78/1.89
$\mu_4\text{-H}_{\text{tet}}$	1.62/1.74
$\mu_3\text{-H}$	1.69/1.71/1.77

Polyhydrido Copper Cluster Model

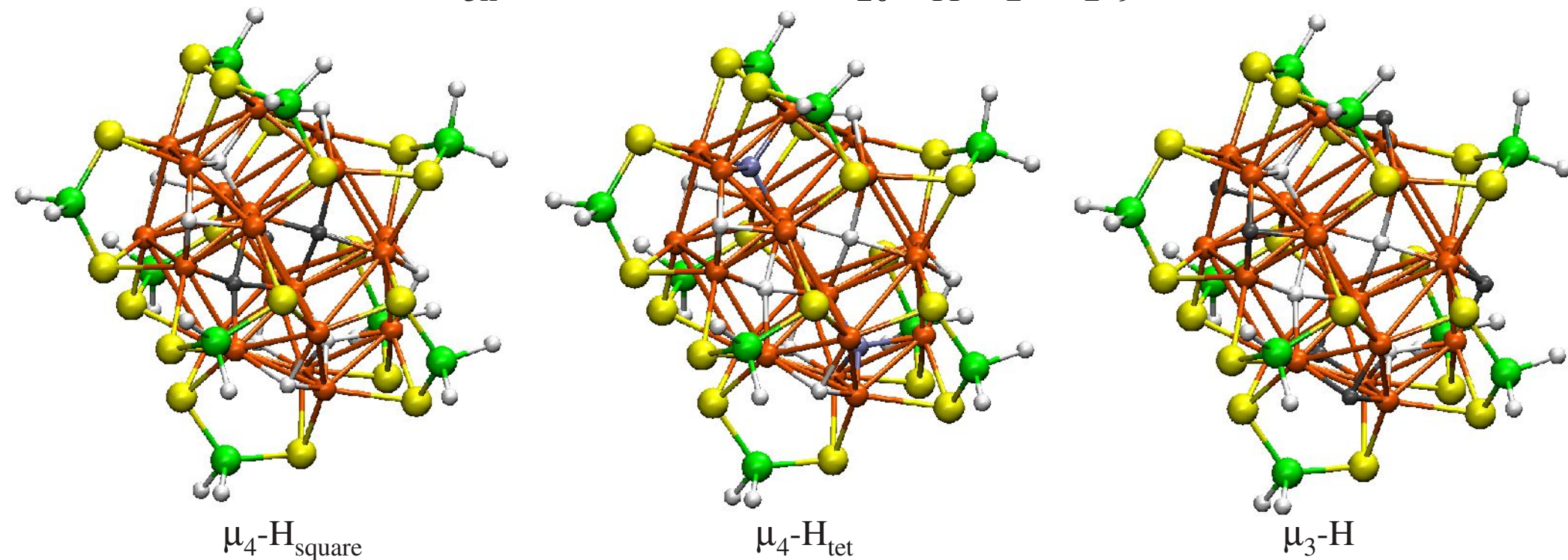
deMon2k
density of Montréal

Optimization & Frequency Analysis: BP86/Def2-TZVP/GEN-A2*



^1H NMR Shielding in Polyhydrido Copper Cluster

$\text{C}_{3\text{h}}$ Model System $\text{Cu}_{20}\text{H}_{11}[\text{S}_2\text{PH}_2]_9$



Chemical Shifts [ppm] with respect to TMS

	Experiment	PBE/aug-cc-pVDZ/GEN-A2*			
Hydrogen	CDCl_3	Tol-d_8	Crystal	Full	Model
$\mu_4\text{-H}_{\text{square}}$	2.80	3.32	4.22, 4.66	4.21, 4.60	4.09
$\mu_4\text{-H}_{\text{tet}}$	1.46	1.88	1.89	2.59, 2.70	1.68
$\mu_3\text{-H}$	-0.99	-0.55	-0.68, -2.04	-0.36, -0.87	-1.66

GIAO-ADFT Magnetic Property Calculation

- Shielding tensor elements

$$\sigma_{xy}(\vec{C}) = \lim_{\vec{H} \rightarrow 0, \vec{M}_c \rightarrow 0} \frac{\partial^2 E}{\partial H_x \partial M_{Cy}} = \sum_{a,b} P_{ab} H_{ab}^{(x,y)}(\vec{C}) + \sum_{a,b} P_{ab}^{(x)} H_{ab}^{(y)}(\vec{C})$$

- Induced magnetic field (IMF)

$$\vec{B}(\vec{R}) = -\boldsymbol{\sigma}(\vec{R}) \vec{H}$$

$\vec{B}(\vec{R})$: induced mag. field at position \vec{R}

\vec{H} : homogeneous external mag. field



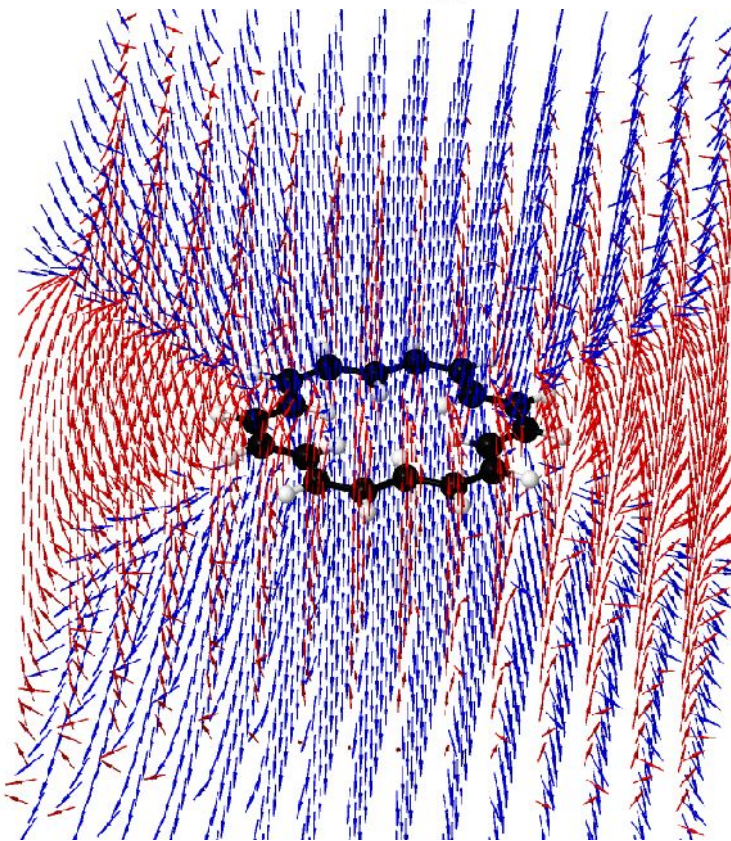
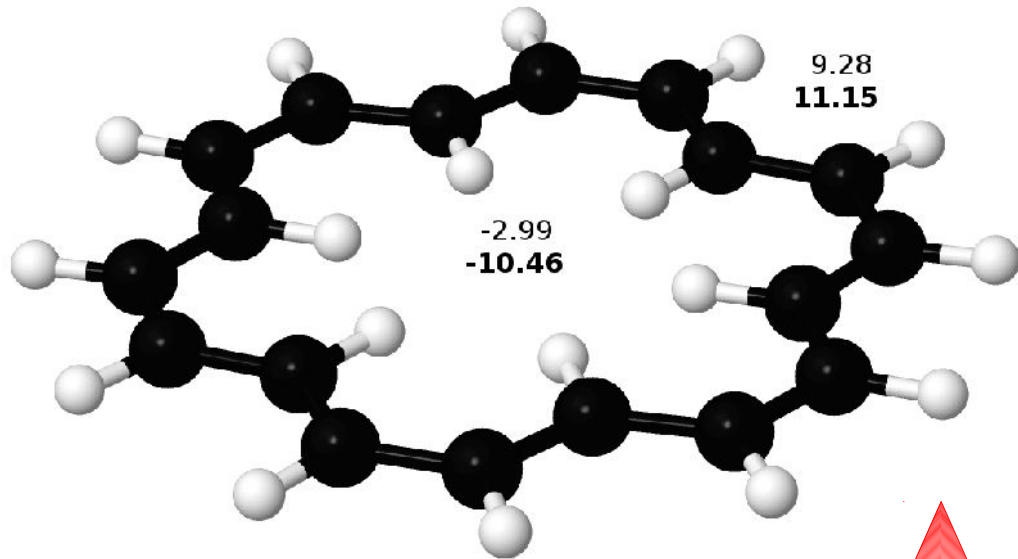
- Magnetic induced current (MIC) density

$$\vec{B}(\vec{R}) = -\frac{1}{c^2} \int \frac{\vec{R} - \vec{R}'}{|\vec{R} - \vec{R}'|^3} \times J(\vec{R}') d\vec{R}'$$

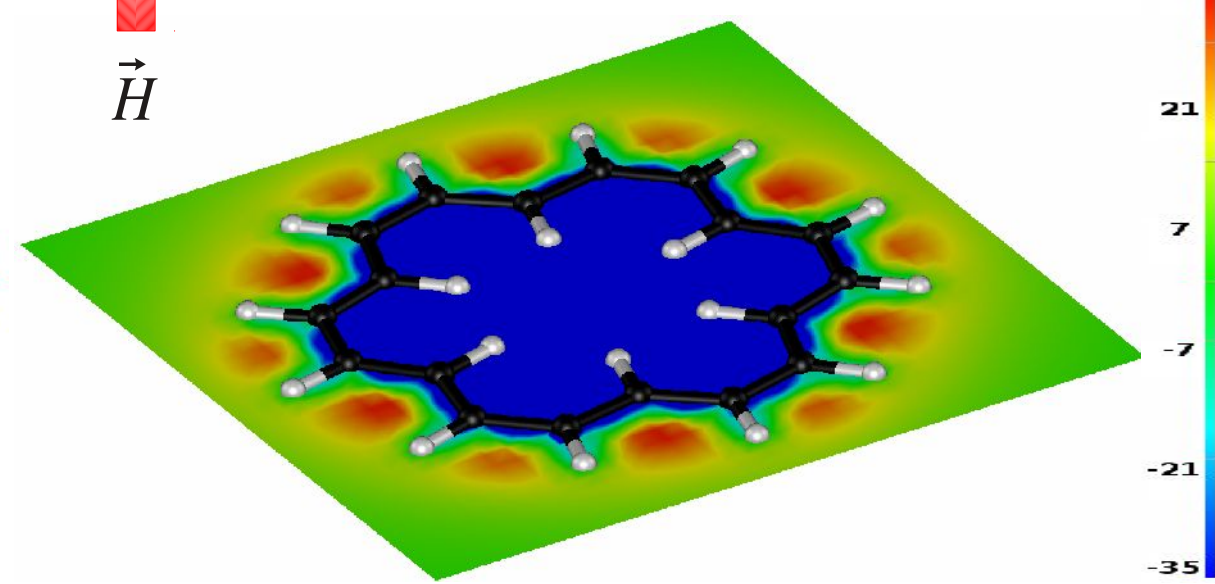
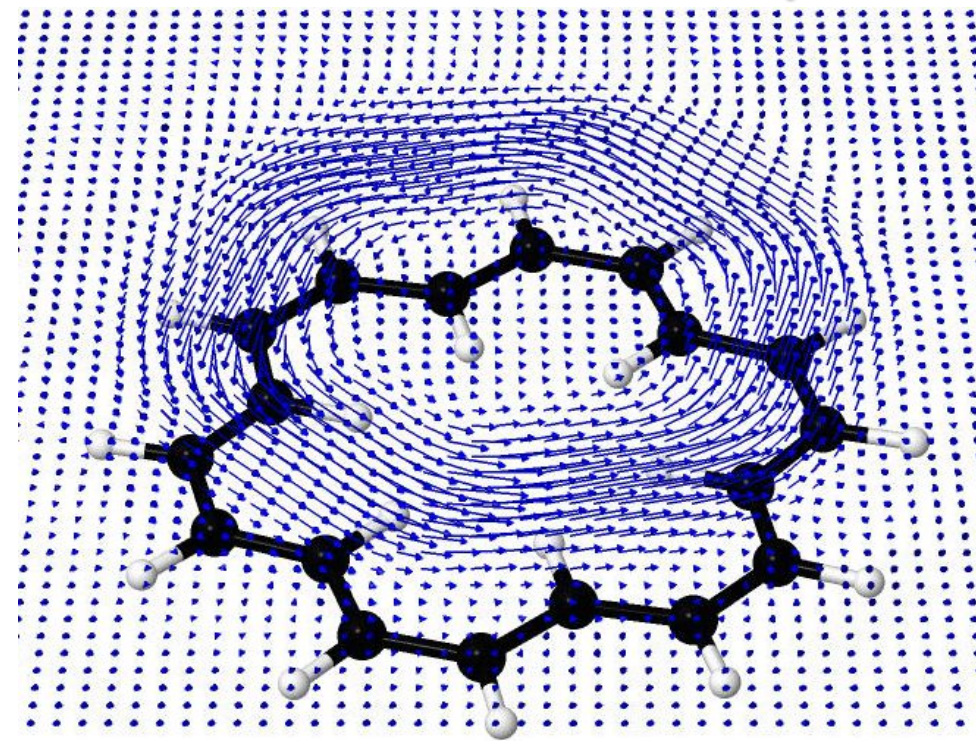


- B. Zuniga-Gutierrez, G. Geudtner, A.M. Köster, *J. Chem. Phys.* **134**, 124108 (2011)
J. Jusélius, D. Sundholm, J. Gauss, *J. Chem. Phys.* **121**, 3952 (2004)
G. Merino, T. Heine, G. Seifert, *Chem. Eur. J.* **10**, 4367 (2004)

Example: [18] Annulene

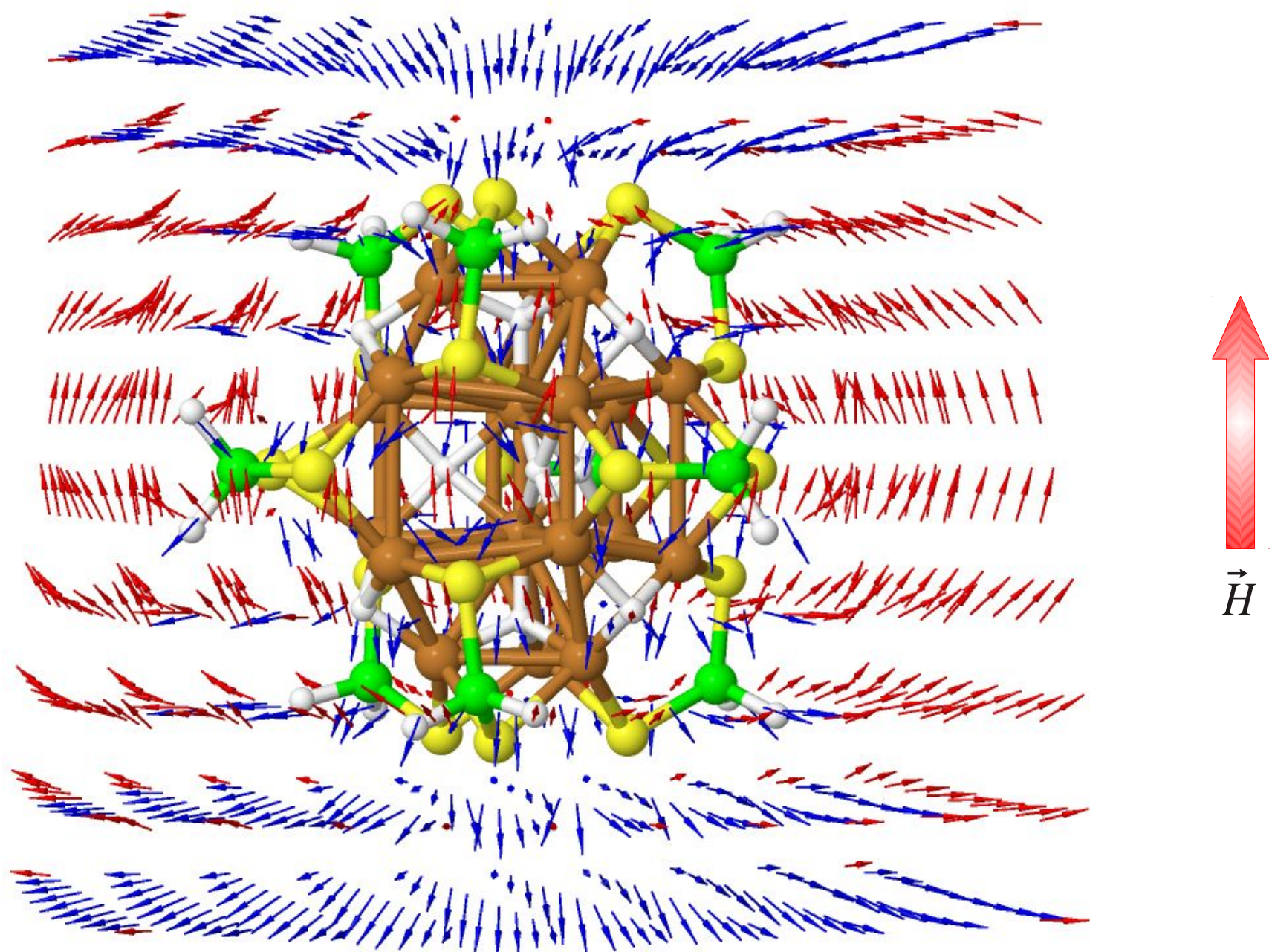


\vec{H}



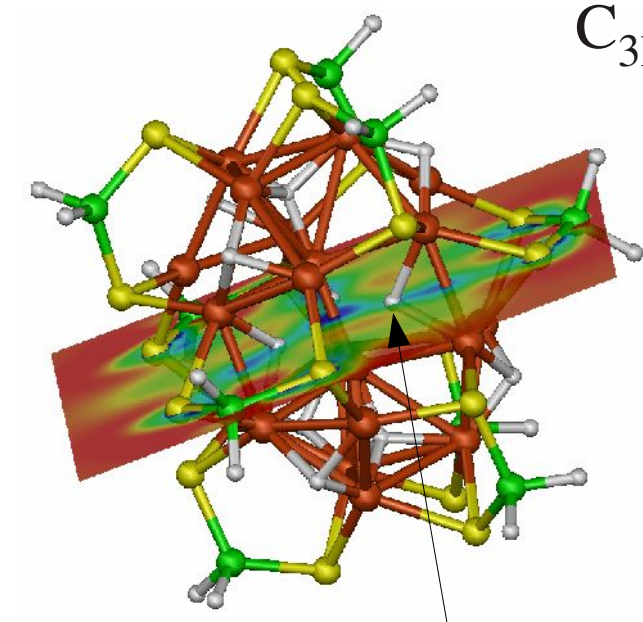
IMF in Polyhydrido Copper Cluster

C_{3h} Model System $Cu_{20}H_{11}[S_2PH_2]_9$



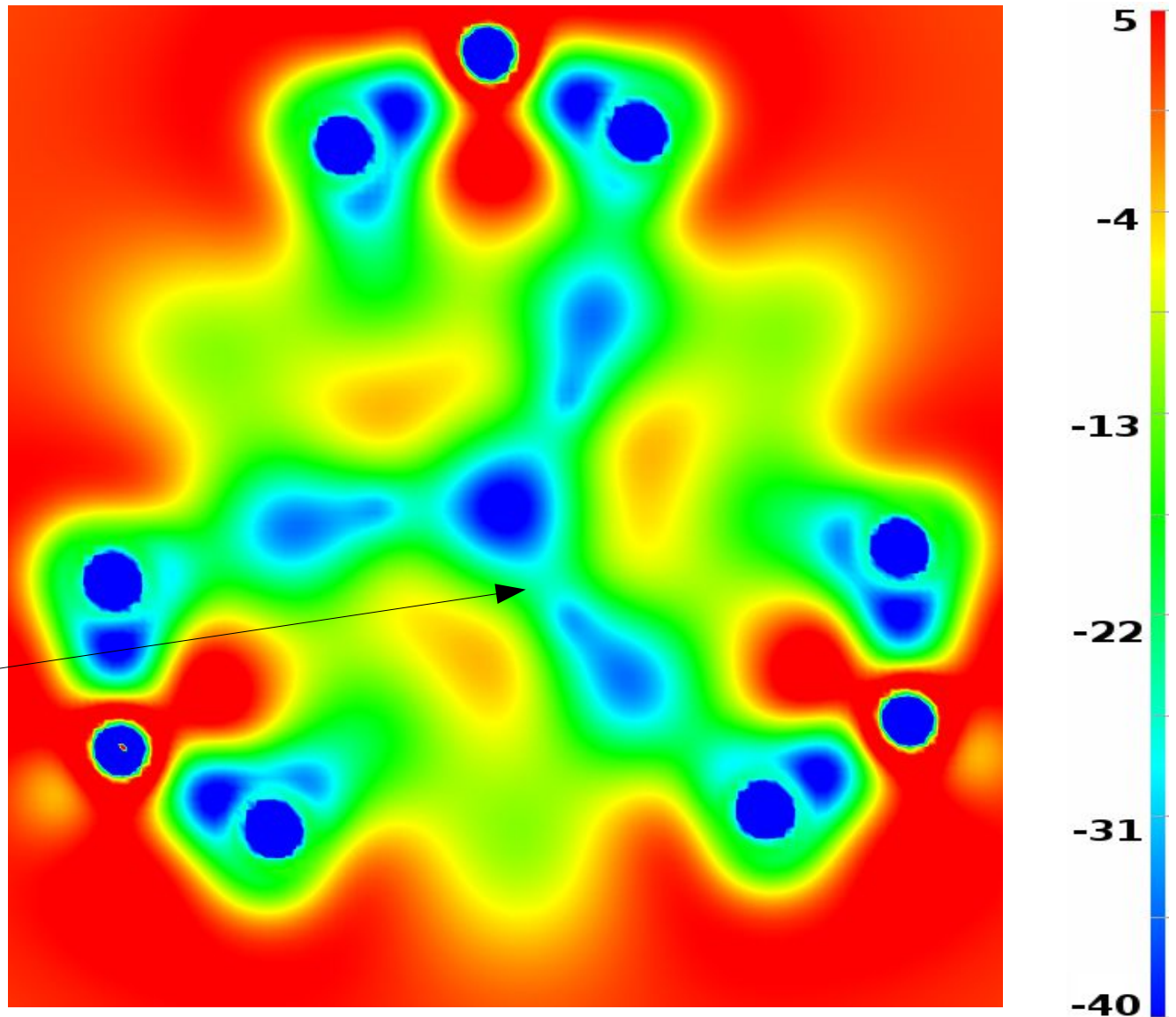
IMF in Polyhydrido Copper Cluster

C_{3h} Model System Cu₂₀H₁₁[S₂PH₂]₉



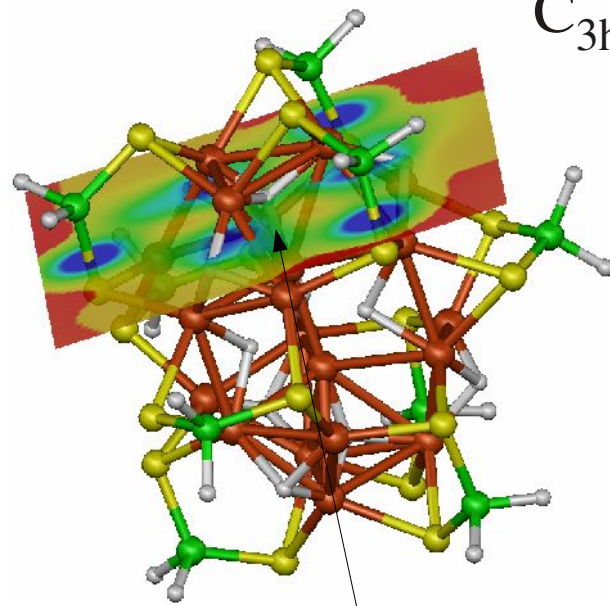
$\mu_4\text{-H}_{\text{square}}$

$\sigma = 4.09 \text{ ppm}$



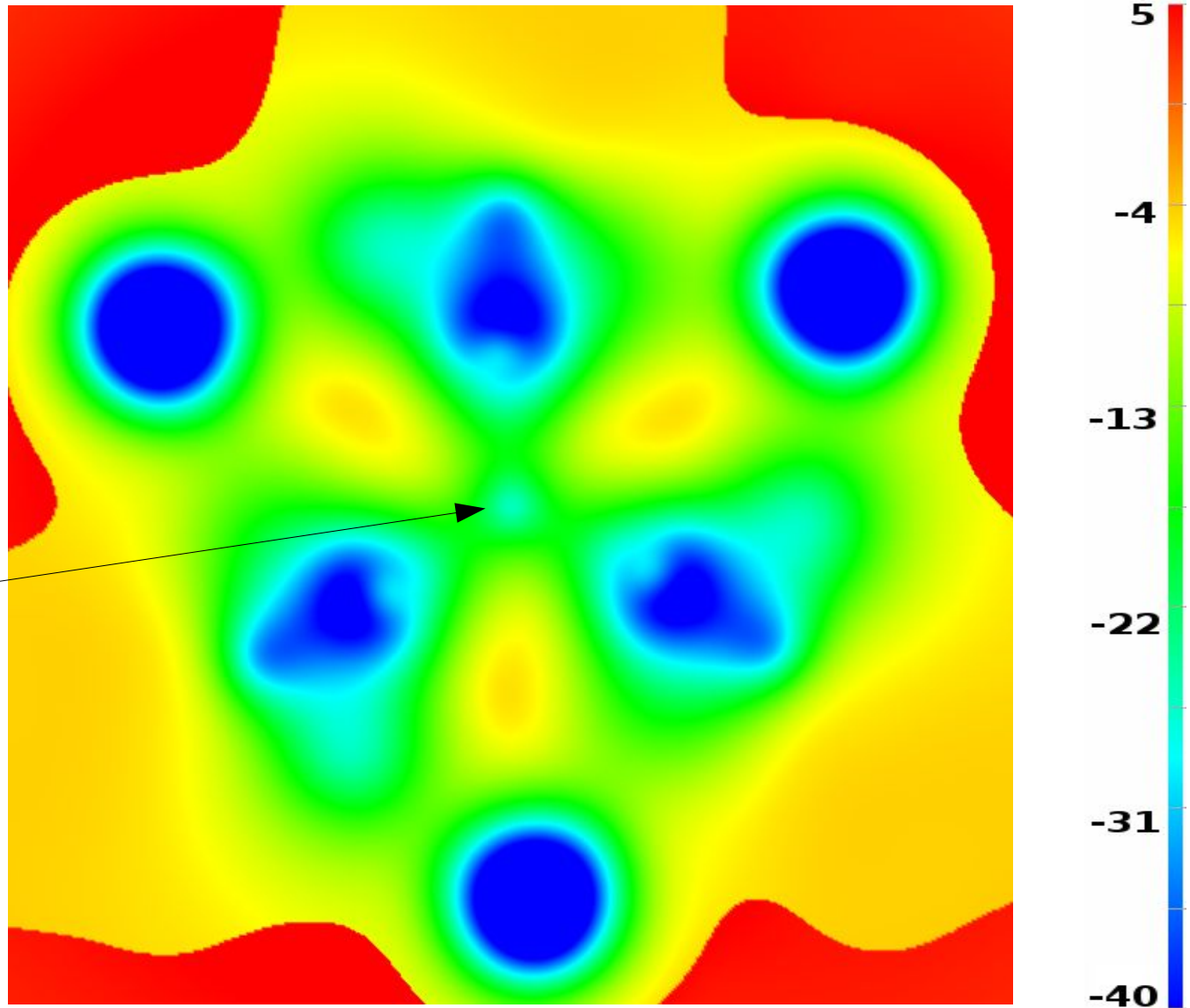
IMF in Polyhydrido Copper Cluster

C_{3h} Model System Cu₂₀H₁₁[S₂PH₂]₉



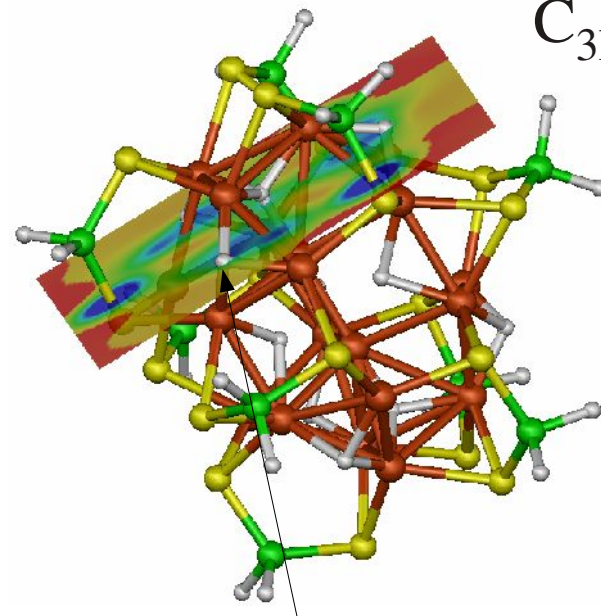
$\mu_4\text{-H}_{\text{tet}}$

$\sigma = 1.68 \text{ ppm}$



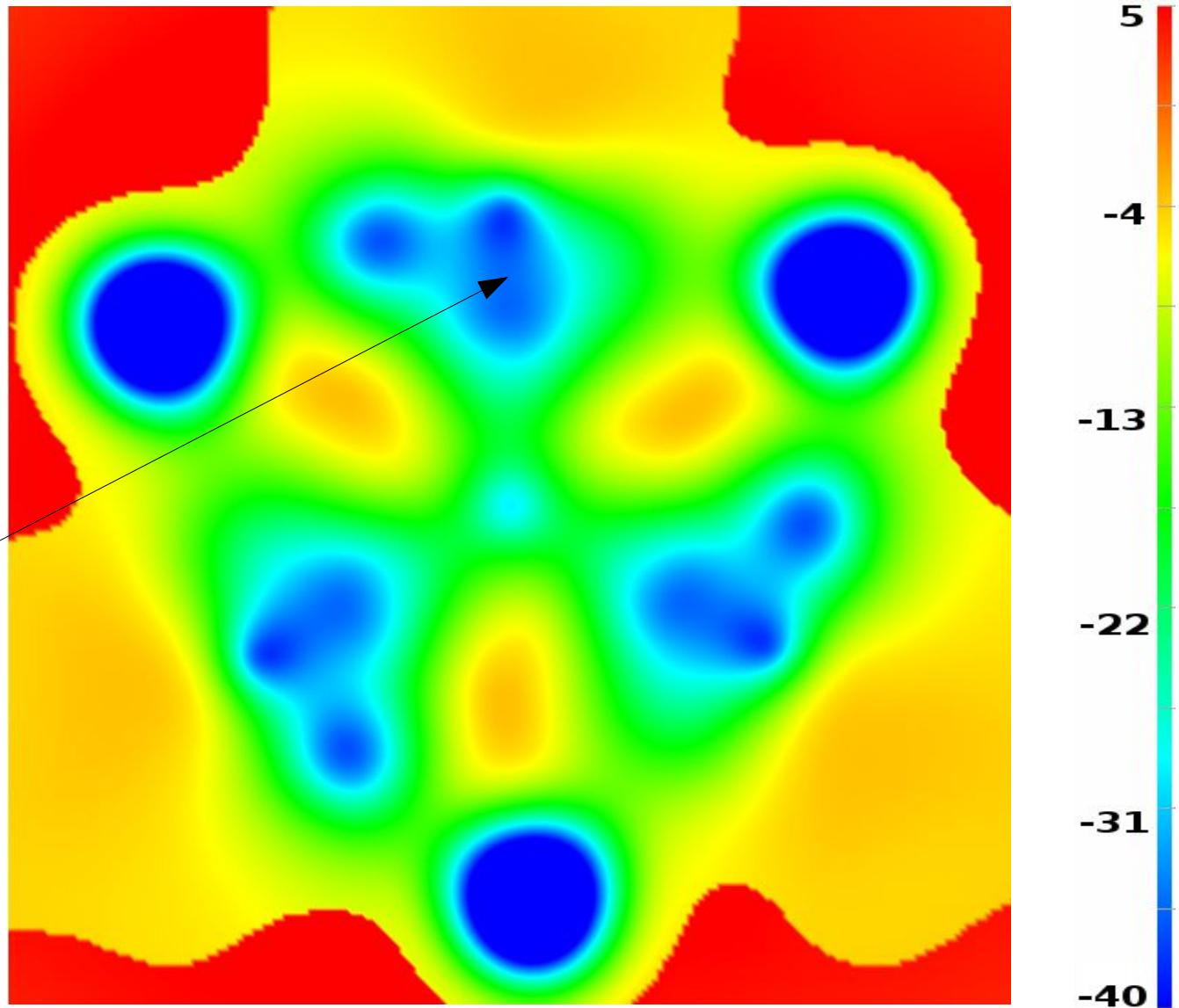
IMF in Polyhydrido Copper Cluster

C_{3h} Model System Cu₂₀H₁₁[S₂PH₂]₉



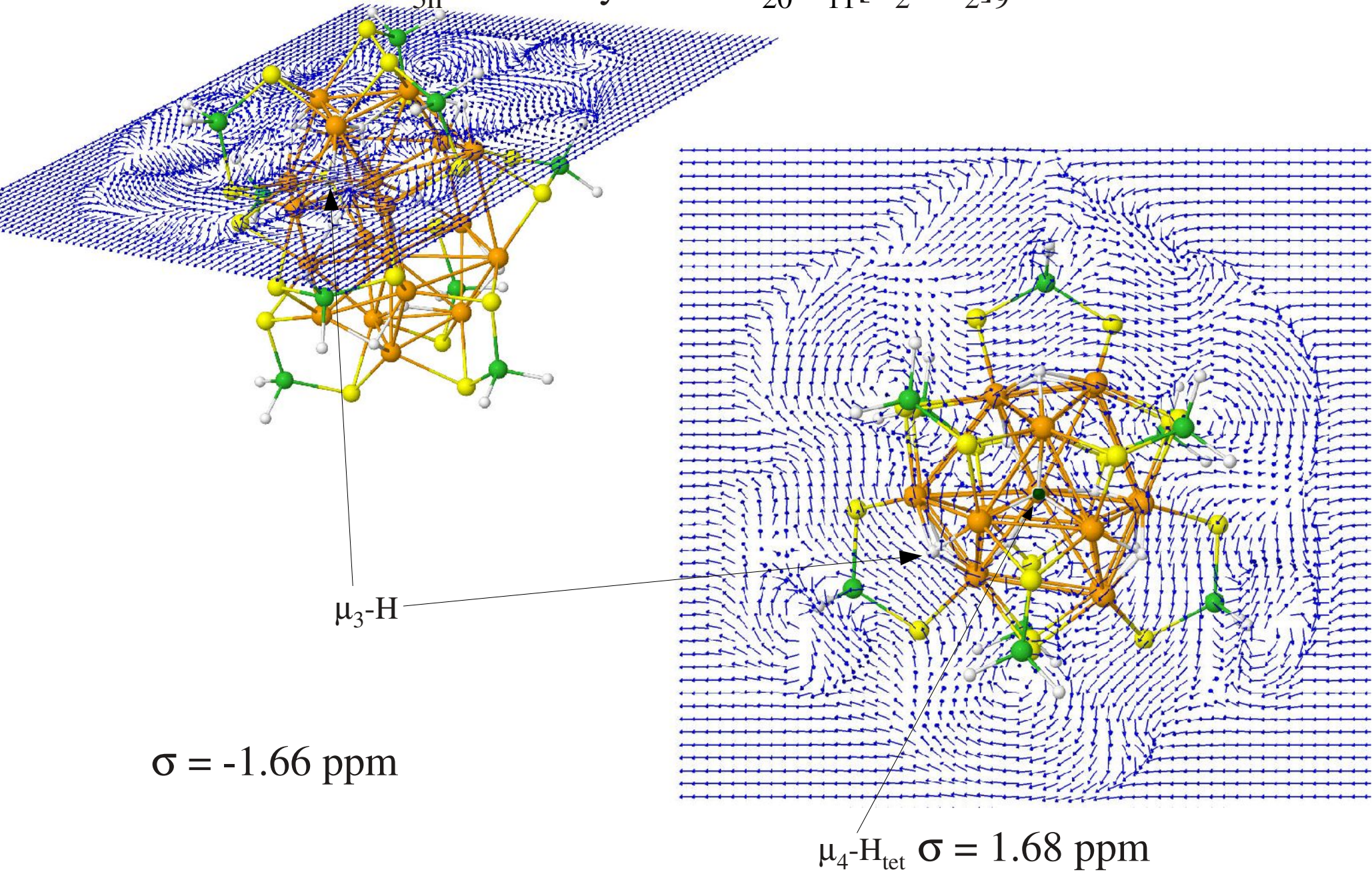
$\mu_3\text{-H}$

$\sigma = -1.66 \text{ ppm}$



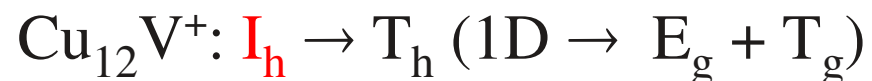
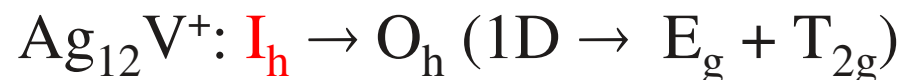
MIC in Polyhydrido Copper Cluster

C_{3h} Model System Cu₂₀H₁₁[S₂PH₂]₉



Conclusions

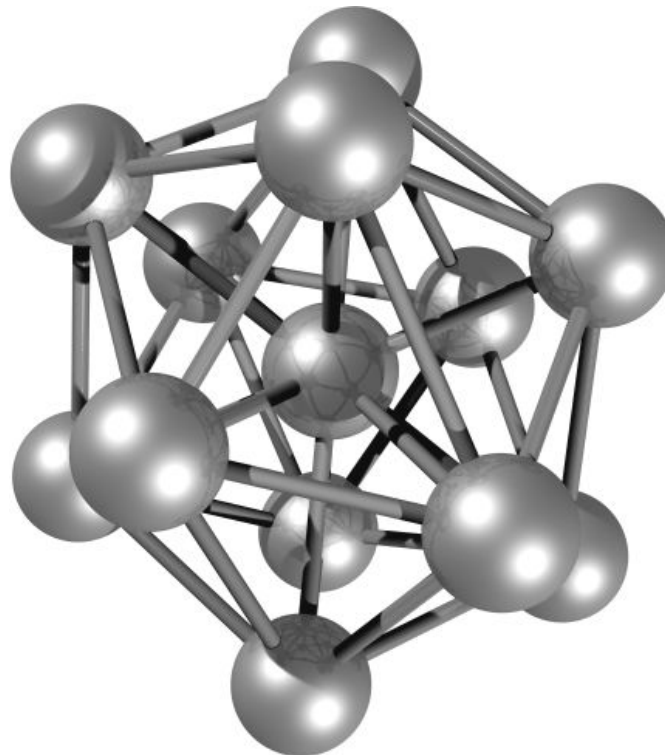
- Hund type cluster ground states are possible for simple metals (Na_{55}^+).
- Local spins can “dissolve” gradually in cluster orbitals ($\text{Cu}_x\text{V}^{0/+}$).
- Simple shell model permits spin and distortion prediction.



- ^1H NMR shielding of interior cluster hydrogens are well reproduced.
- IMF and MIC yield detailed insight of induced magnetic field mechanism.

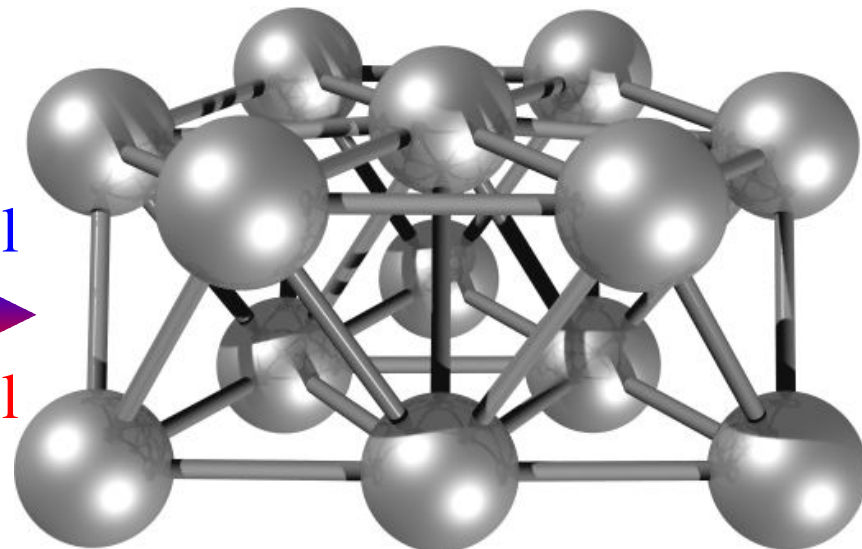
In $\text{Cu}_{20}\text{H}_{11}[\text{S}_2\text{PH}_2]_9$ very different to classical aromatic compounds!

Pd₁₃ Ground State(s)



$$\Delta E \approx 3 \text{ kcal/mol}$$

$$\Delta E \approx 8 \text{ kcal/mol}$$



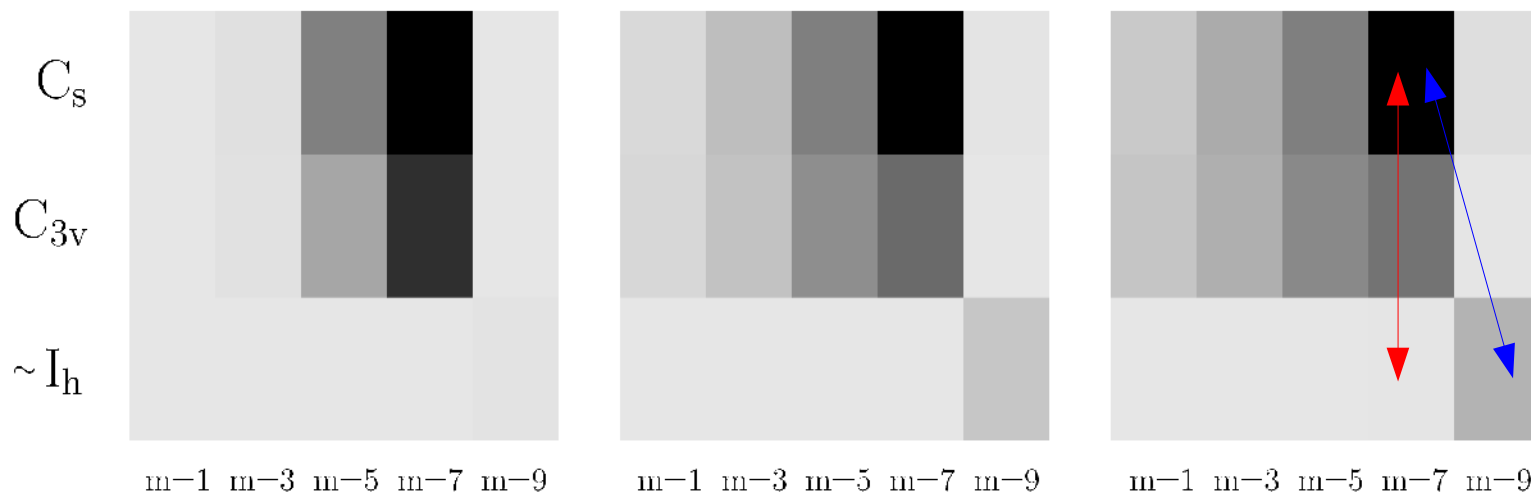
P. Nava, M. Sierka, R. Ahlrichs, *Phys. Chem. Chem. Phys.* **5**, 3372 (2003)
 Y. Sun, M. Zhang, R. Fournier, *Phys. Rev. B* **77**, 075435 (2008)

C.M. Chang, M.Y. Chou, *Phys. Rev. Lett.* **93**, 133401 (2004)
 L.L. Wang, D.D. Johnson, *Phys. Rev. B* **75**, 235405 (2007)
 A.M. Köster et al. *J. Am. Chem. Soc.* **133**, 12192 (2011)

100 K

300 K

500 K



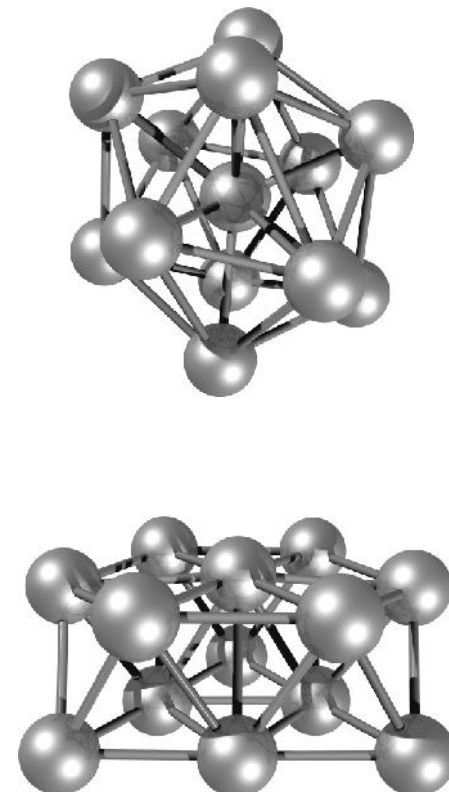
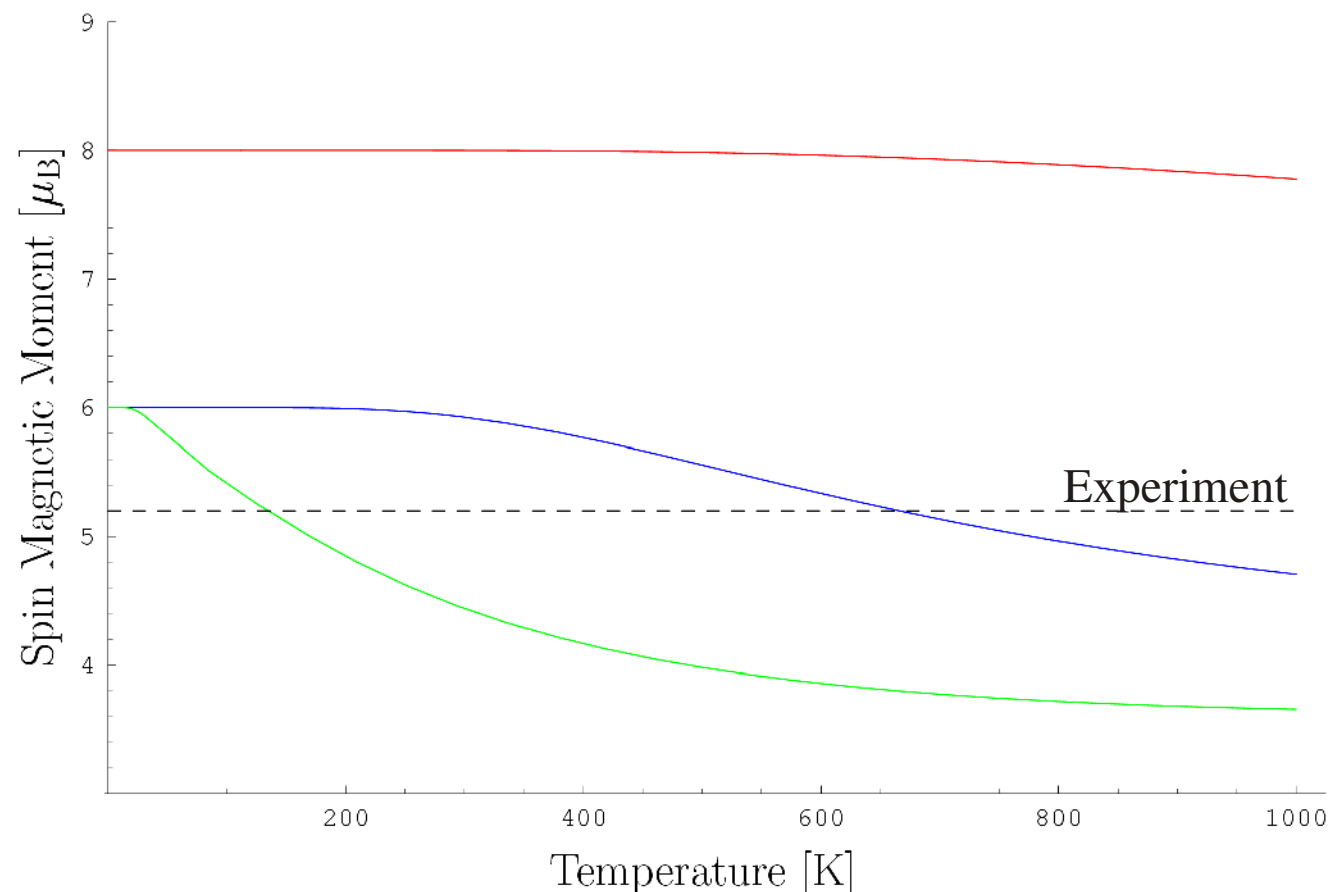
Comparison with Experiment

Experimental spin moment: $5.2 \mu_B$

A.J. Cox, J.G. Louderback, S.E. Apsel, L.A. Bloomfield, *Phys. Rev. B* **49**, 12295 (1994)

Theoretical spin moment averaging:

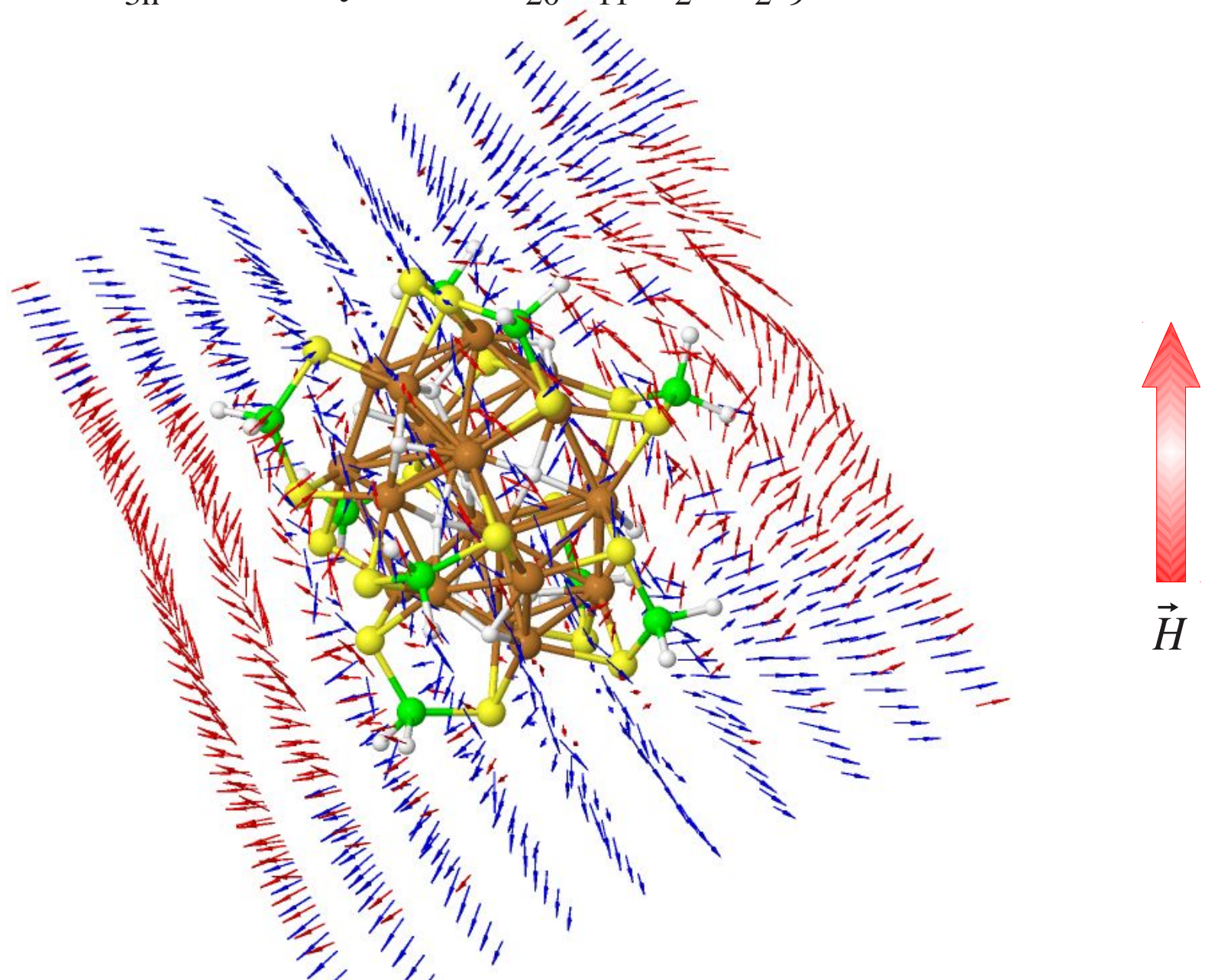
$$\langle \mu(T) \rangle = \sum_{m=1}^9 \frac{e^{-\frac{\Delta \epsilon_m}{RT}}}{Q(T)} (m-1) \mu_B \quad \text{with} \quad Q(T) = \sum_{m=1}^9 e^{-\frac{\Delta \epsilon_m}{RT}}$$



👉 Only bi-layer structure is compatible to experiment!

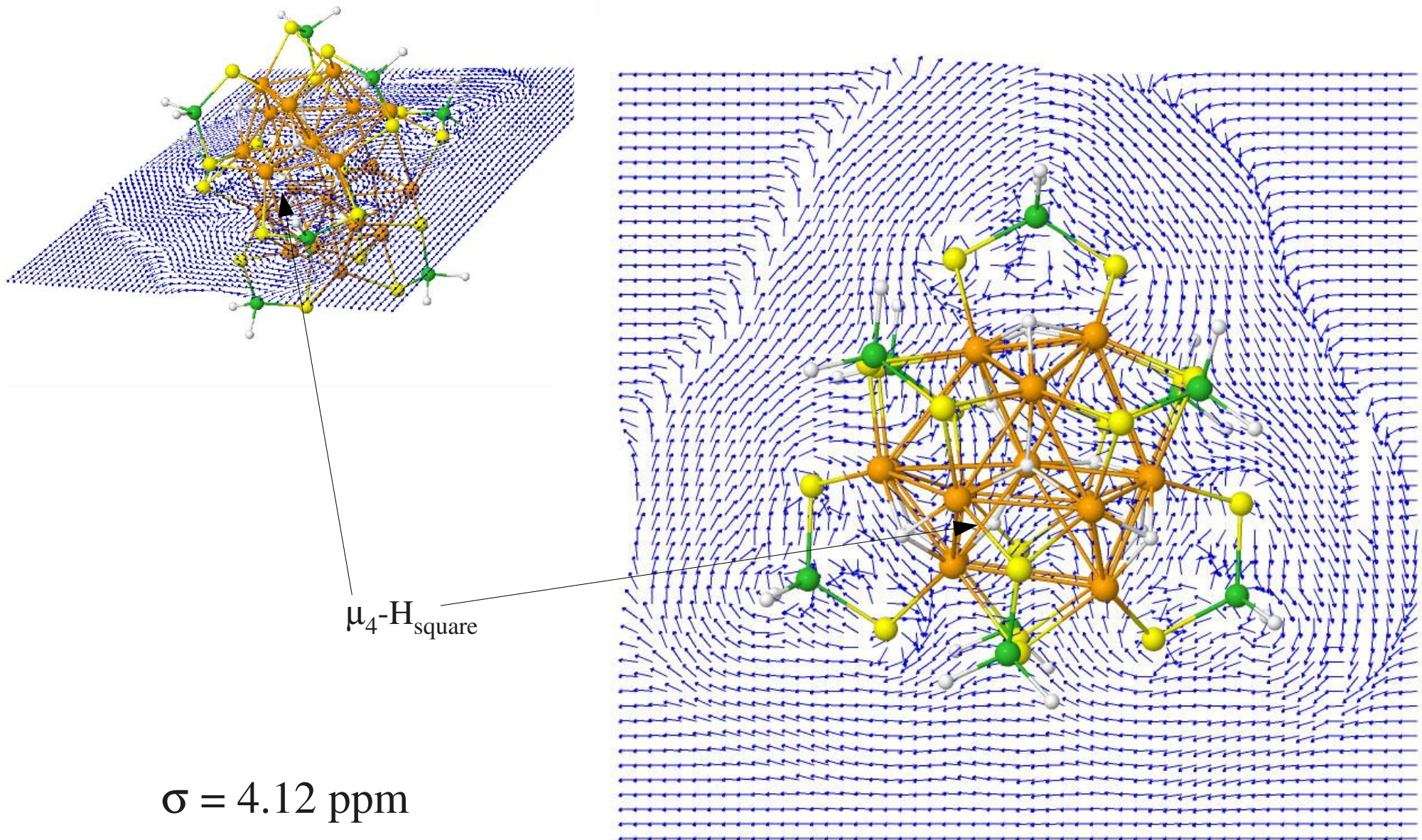
IMF in Polyhydrido Copper Cluster

C_{3h} Model System Cu₂₀H₁₁[S₂PH₂]₉



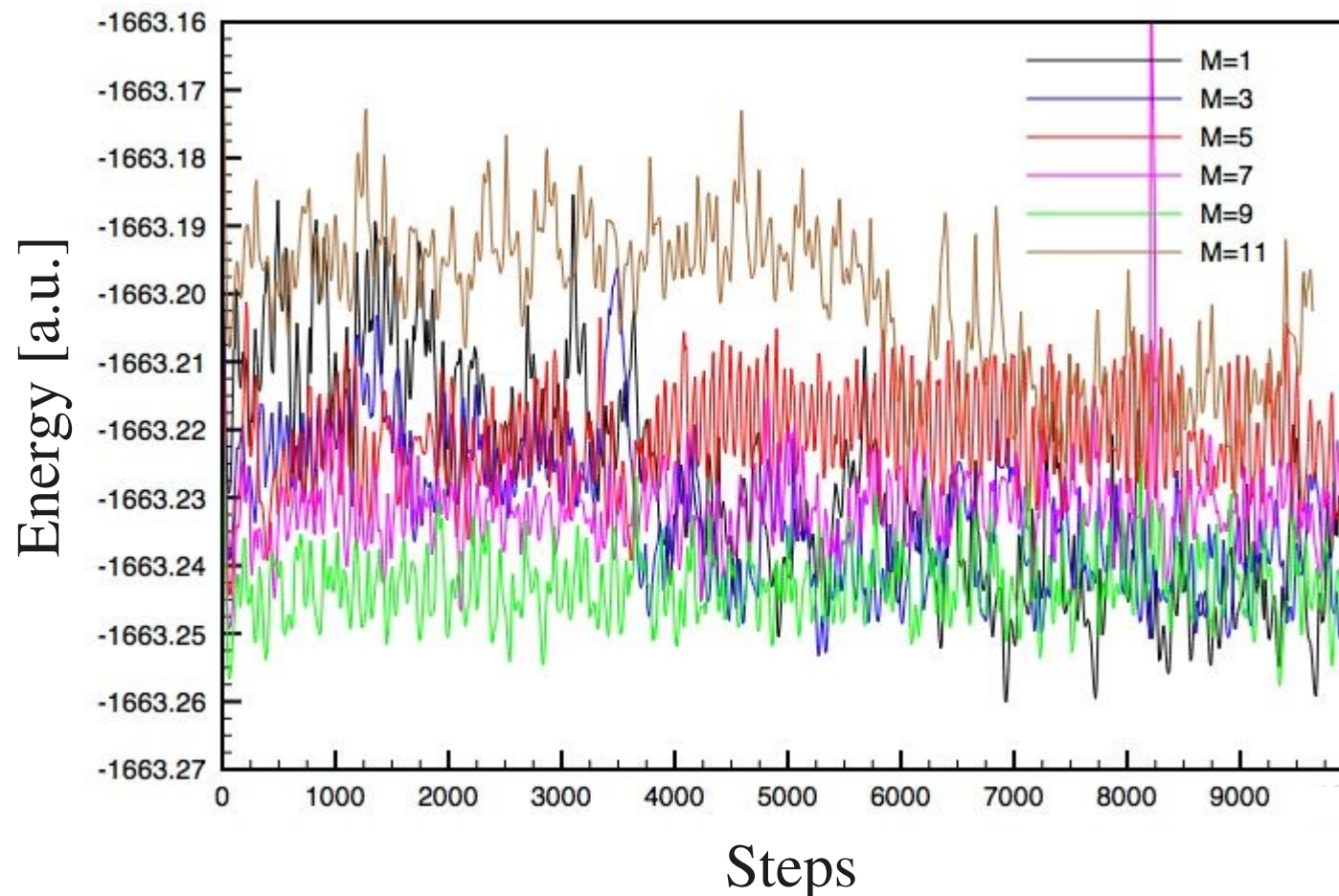
MIC in Polyhydrido Copper Cluster

C_{3h} Model System Cu₂₀H₁₁[S₂PH₂]₉



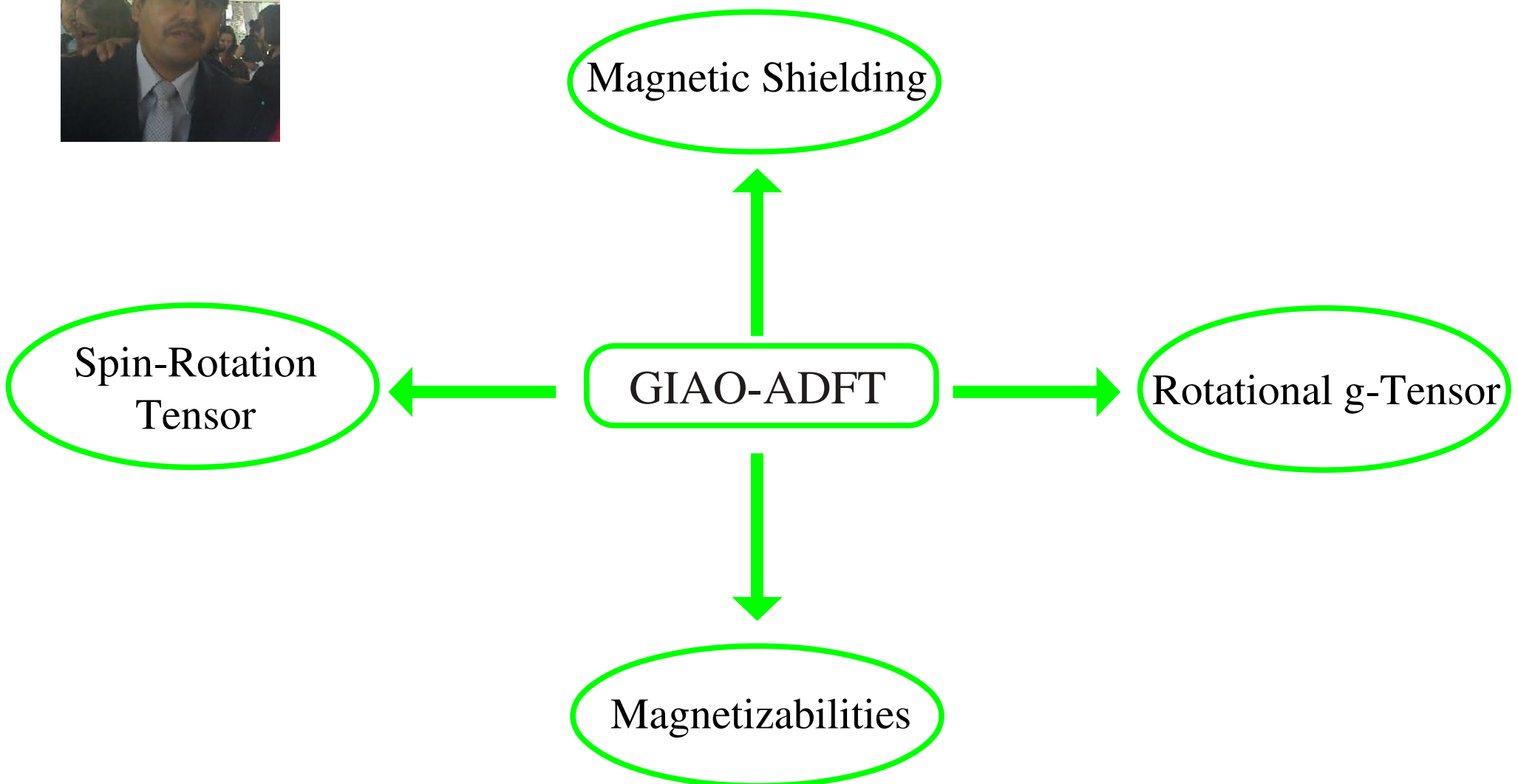
BOMD of Pd₁₃ at 500 K

Are ~I_h Structures Accessible?



⌚ Need LS coupling for BOMD inter system crossings

GIAO-ADFT



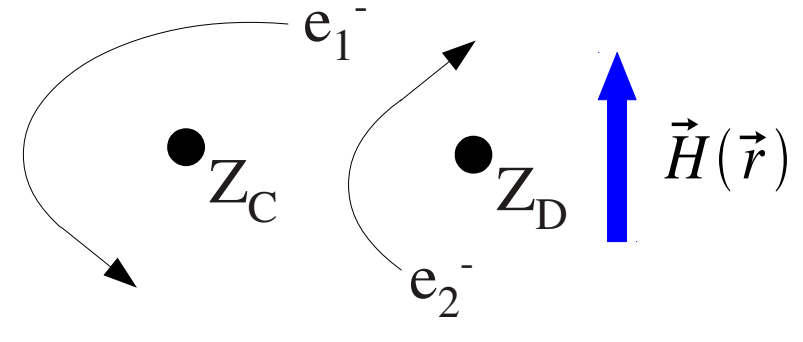
Classical Phenomenological Hamiltonian

Lagrangian [in a.u.] for moving electrons in an electromagnetic field:

$$\mathcal{L}(\vec{r}, \dot{\vec{r}}, t) = \frac{1}{2} \sum_{j=1}^n \dot{\vec{r}}_j^2 + \phi(\vec{r}_j) - \dot{\vec{r}}_j \cdot \vec{\mathcal{A}}(\vec{r}_j)$$

Born-Oppenheimer approximation:

$$\phi(\vec{r}_j) = - \sum_{C=1}^N \frac{Z_C}{|\vec{r}_j - \vec{C}|} + \frac{1}{2} \sum_{k \neq j}^n \frac{1}{|\vec{r}_j - \vec{r}_k|}$$



Hamiltonian [in a.u.] for moving electrons in an electromagnetic field:

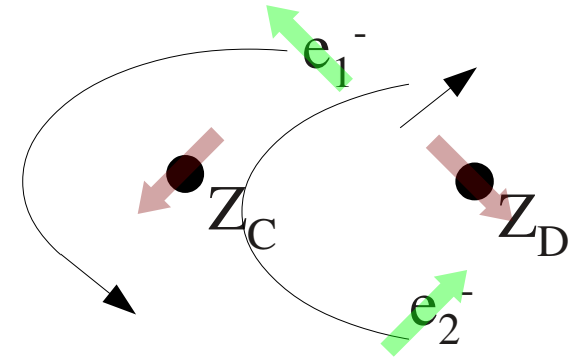
$$\mathcal{H}(\vec{r}, \vec{\pi}, t) = \frac{1}{2} \sum_{j=1}^n \left[\vec{\pi}_j + \vec{\mathcal{A}}(\vec{r}_j) \right]^2 + \sum_{j=1}^n \phi(\vec{r}_j)$$

$$\vec{\pi}_j = \frac{\partial \mathcal{L}}{\partial \dot{\vec{r}}_j} = \dot{\vec{r}}_j - \vec{\mathcal{A}}(\vec{r}_j)$$

Classical Phenomenological Hamiltonian

Adding of particle spins ↗ Pauli-type Hamiltonian:

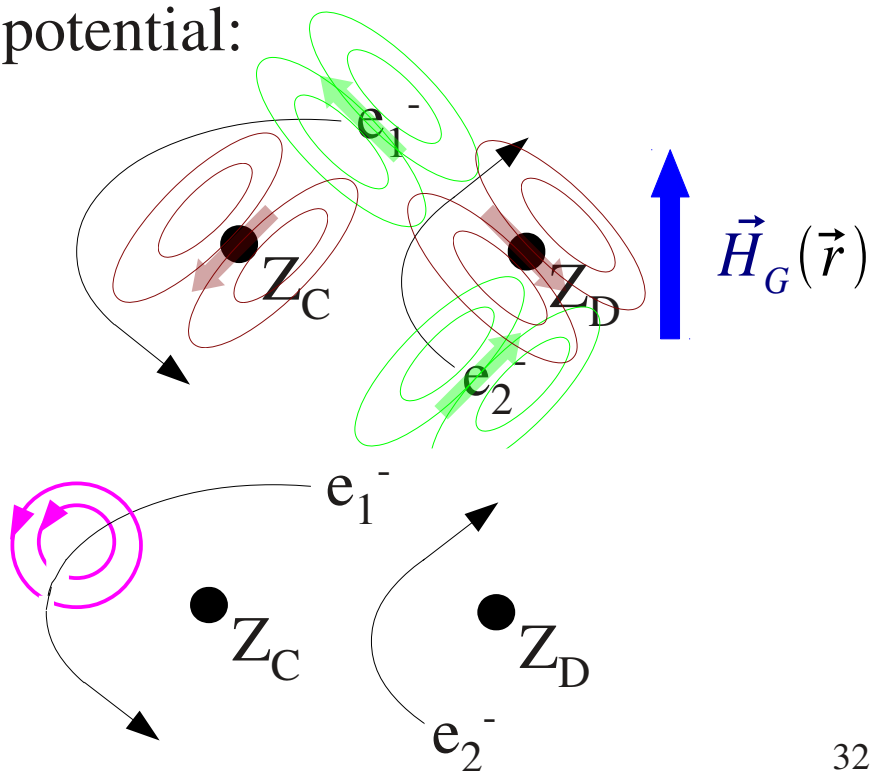
$$\mathcal{H}(\vec{r}, \vec{\pi}, t) = \frac{1}{2} \sum_{j=1}^n \left[\vec{\pi}_j + \vec{\mathcal{A}}(\vec{r}_j) \right]^2 + \sum_{j=1}^n \phi(\vec{r}_j) - \sum_{j=1}^n \vec{M}_e \cdot \vec{H}(\vec{r}_j) - \sum_{C=1}^N \vec{M}_C \cdot \vec{H}(\vec{C})$$



Expansion of local magnetic field and vector potential:

$$\vec{H}(\vec{r}) = \vec{H}_G(\vec{r}) \sum_{j=1}^n \sum_{j=1}^n (\vec{H}_j)(\vec{r}) + \sum_{C=1}^N \sum_{C=1}^N (\vec{H}_C)(\vec{r})$$

$$\vec{\mathcal{A}}_G \vec{\mathcal{A}}_D(\vec{r}) = \frac{1}{2} \frac{1}{2} \vec{H}_G \vec{H}_G \times (\vec{r} \vec{G} \vec{G})$$



$$\vec{\mathcal{A}}(\vec{r}) = \vec{\mathcal{A}}_G(\vec{r}) + \sum_{j=1}^n \vec{\mathcal{A}}_j(\vec{r}) + \sum_{C=1}^N \vec{\mathcal{A}}_C(\vec{r})$$

Classical Phenomenological Hamiltonian

Hamiltonian after magnetic field/vector potential expansion:

$$\begin{aligned}
 \mathcal{H}(\vec{r}, \vec{\pi}, t) = & \frac{1}{2} \sum_{j=1}^n \vec{\pi}_j^2 + \varphi(\vec{r}_j) \boxed{\vec{H} \cdot \vec{\chi}^{para}} + \sum_{j=1}^n \vec{M}_e \cdot \vec{\sigma}^{para}(\vec{r}_j) + \sum_{C=1}^N \vec{M}_C \cdot \vec{\sigma}^{para}(\vec{C}) + \\
 & \boxed{\vec{H} \cdot \vec{\chi}^{dia} \cdot \vec{H} + \sum_{C=1}^N \vec{H} \cdot \vec{\sigma}^{dia}(\vec{C}) \cdot \vec{M}_C + \sum_{j=1}^n \vec{H} \cdot \vec{g}^{dia}(\vec{r}_j) \cdot \vec{M}_e} + \\
 & \sum_{C=1}^N \sum_{D>C}^N \vec{M}_C \cdot \vec{I}_{CD}^{dso} \cdot \vec{M}_C + \sum_{j=1}^n \sum_{k>j}^n \vec{M}_e \cdot \vec{I}_{jk}^{dso} \cdot \vec{M}_e + \sum_{C=1}^N \sum_{j=1}^n \vec{M}_C \cdot \vec{I}_{Cj}^{dso} \cdot \vec{M}_e - \\
 & \sum_{j=1}^n \vec{H} \cdot \vec{M}_e + \sum_{j=1}^n \sum_{k>j}^n \vec{M}_e \cdot \vec{I}_{jk}^{dir} \cdot \vec{M}_e + \sum_{j=1}^n \sum_{k>j}^n \vec{M}_e \cdot \vec{I}_{jk}^{Fc} \cdot \vec{M}_e - \\
 & \sum_{C=1}^N \vec{H} \cdot \vec{M}_C + \sum_{C=1}^N \sum_{D>C}^N \vec{M}_C \cdot \vec{I}_{CD}^{dir} \cdot \vec{M}_D + \sum_{C=1}^N \sum_{j=1}^n \vec{M}_C \cdot \vec{I}_{Cj}^{Fc} \cdot \vec{M}_e + \\
 & \sum_{C=1}^N \sum_{j=1}^n \vec{M}_C \cdot \vec{I}_{Cj}^{dir} \cdot \vec{M}_e
 \end{aligned}$$

Gauge-Including Atomic Orbitals (GIAO)

GIAO Function:

$$\phi_a(\vec{r}, \vec{H}) \equiv a(\vec{r}) e^{-\frac{i}{2} (\vec{H} \times (\vec{A}) - \vec{G}) \cdot \vec{r}} \simeq a(\vec{r}) \frac{i}{2} (\vec{H} \vec{H} \vec{A} (\vec{A} \vec{r} \cdot \vec{G}) \vec{r} \cdot \vec{G}) a(\vec{r})$$

Density:

$$\rho(\vec{r}, \vec{H}) = \sum_a^{\text{occ}} \phi_a^*(\vec{r}, \vec{H}) \phi_a(\vec{r}, \vec{H}) = \sum_a^{\text{occ}} a(\vec{r}) a(\vec{r}) = \rho(\vec{r})$$

Density response:

$$\frac{\partial \rho(\vec{r}, \vec{H})}{\partial H_x} = \frac{\partial \rho(\vec{r})}{\partial H_x} = 0 \quad \Rightarrow \quad \frac{\partial \tilde{\rho}(\vec{r}, \vec{H})}{\partial H_x} = \frac{\partial \tilde{\rho}(\vec{r})}{\partial H_x} = 0$$

Kinetic energy density:

$$\tau = \frac{1}{2} \sum_j^{\text{occ}} \left[i \vec{\nabla} \psi_j(\vec{r}) \right] \cdot \left[-i \vec{\nabla} \psi_j(\vec{r}) \right]$$

$$\tau = \frac{1}{2} \sum_j^{\text{occ}} \left[i \vec{\nabla} + \vec{\mathcal{A}}_G(\vec{r}) \right] \psi_j^*(\vec{r}, \vec{H}) \cdot \left[-i \vec{\nabla} + \vec{\mathcal{A}}_G(\vec{r}) \right] \psi_j(\vec{r}, \vec{H})$$

GIAO-RI-DFT and GIAO-ADFT Shielding Tensor

$$\sigma_{xy}(C) = \lim_{\vec{H} \rightarrow \vec{0}, \vec{M}_C \rightarrow \vec{0}} \frac{\partial^2 E}{\partial H_x \partial M_{Cy}} = \sum_{a,b} P_{ab} H_{ab}^{(x,y)}(C) + \sum_{a,b} P_{ab}^{(x)} H_{ab}^{(y)}(C)$$

GIAO-RI-DFT Perturbed Kohn-Sham Matrix:

$$K_{ab}^{(x)} \equiv \frac{\partial K_{ab}}{\partial H_x} = H_{ab}^{(x)} + \sum_{\bar{k}} \langle \phi_a^* \phi_b \| \bar{k} \rangle^{(x)} x_{\bar{k}} + \langle \phi_a^* | v_{xc}[\rho] | \phi_b \rangle^{(x)}$$

GIAO-ADFT Perturbed Kohn-Sham Matrix:

$$K_{ab}^{(x)} \equiv \frac{\partial K_{ab}}{\partial H_x} = H_{ab}^{(x)} + \sum_{\bar{k}} \langle \phi_a^* \phi_b \| \bar{k} \rangle^{(x)} (x_{\bar{k}} + z_{\bar{k}}) ; \quad z_{\bar{k}} = \sum_{\bar{l}} \langle \bar{k} \| \bar{l} \rangle \langle \bar{l} | v_{xc}[\tilde{\rho}] \rangle$$

New GIAO Integral Recurrence Relation (like for ERIs):

Instead of independent P_{ab} and $H_{ab}^{(x,y)}(C)$ building, build directly the expectation value $\sigma_{xy}^D(C) = \sum_{a,b} P_{ab} H_{ab}^{(x,y)}(C)$!

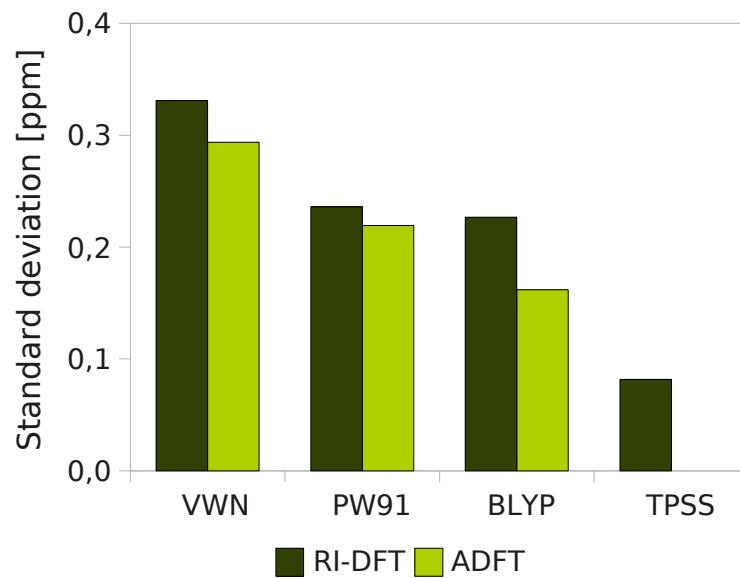
Validation of GIAO-ADFT Shielding Tensor Calculation

- 16 molecules whose experimental chemical shifts are determined in gas phase.
- The VWN/DZVP/A2 optimized structures are used for the NMR calculation.
- References: Methane for C and H; Ammonia for N; Water for O.
- HF and MP2 references used MP2/tz2p optimized structures and the qz2p basis set for the NMR calculation. We used aug-cc-pVQZ basis set for the NMR calculations.

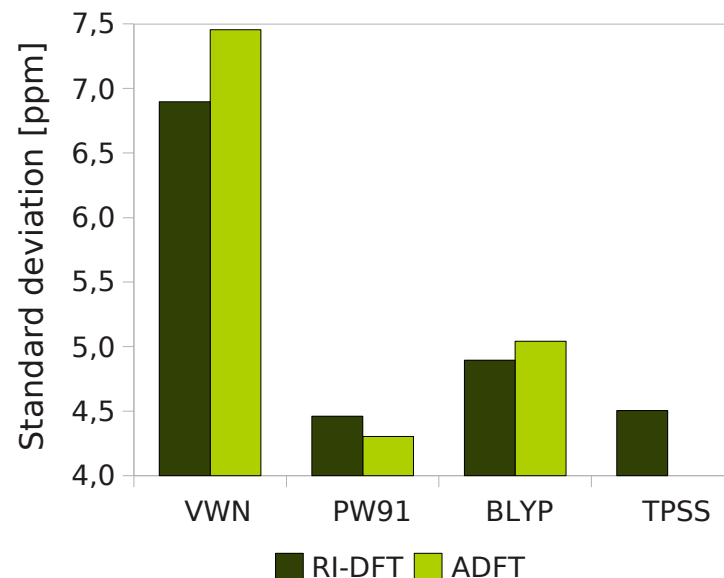
B. Zuniga-Gutierrez, G. Geudtner, A.M. Köster, *J. Chem. Phys.* **134**, 124108 (2011)

GIAO-ADFT vs. GIAO-RI-DFT Shielding Tensor

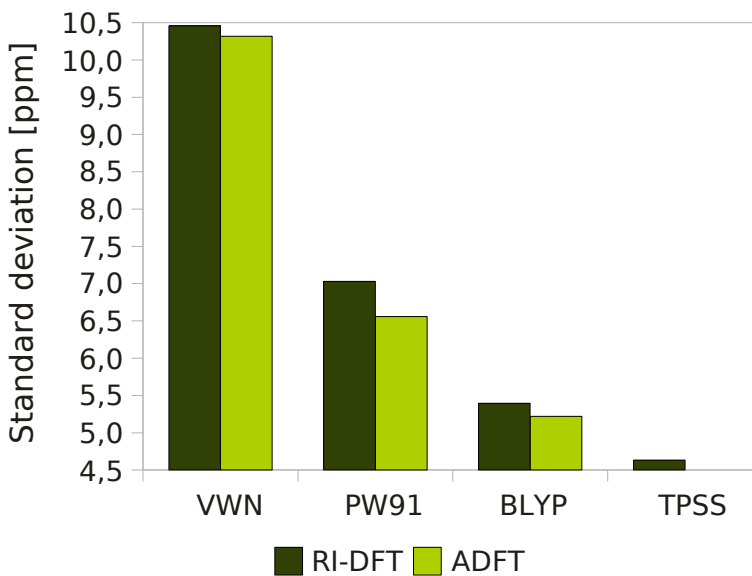
Hydrogen



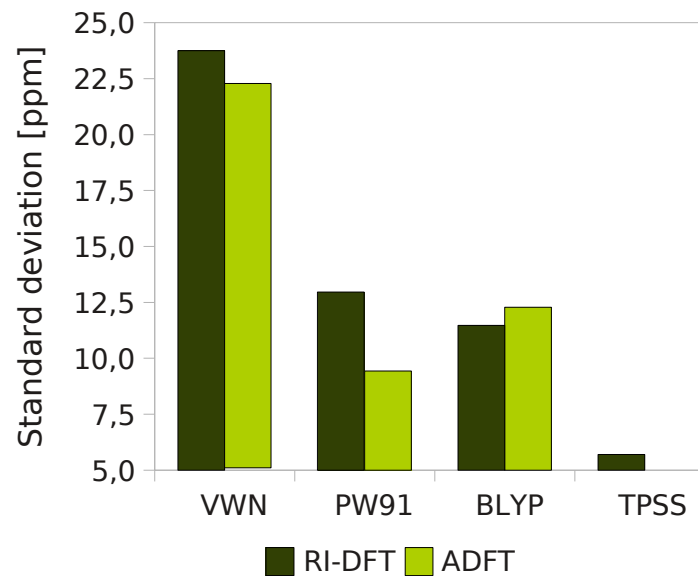
Carbon



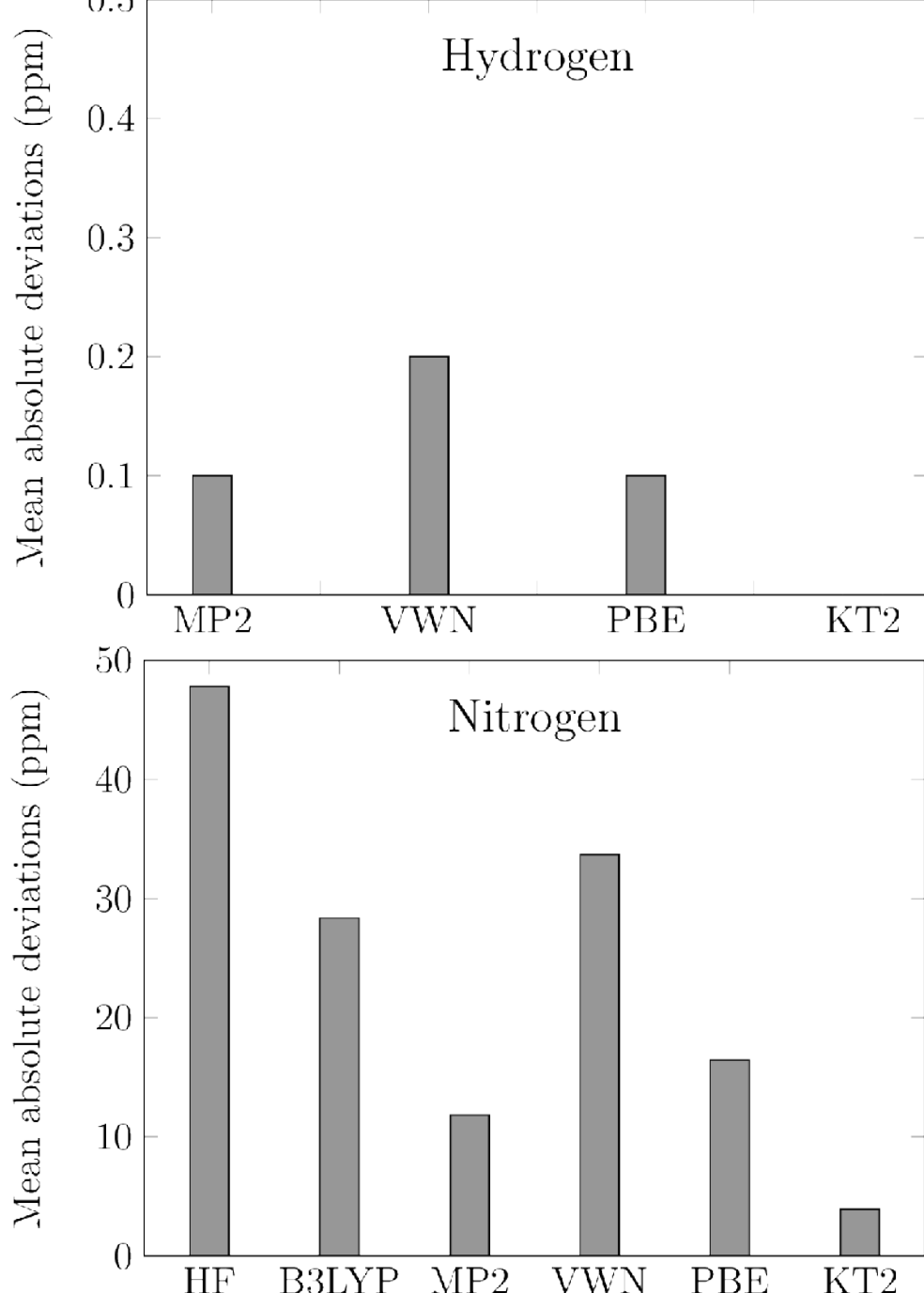
Nitrogen



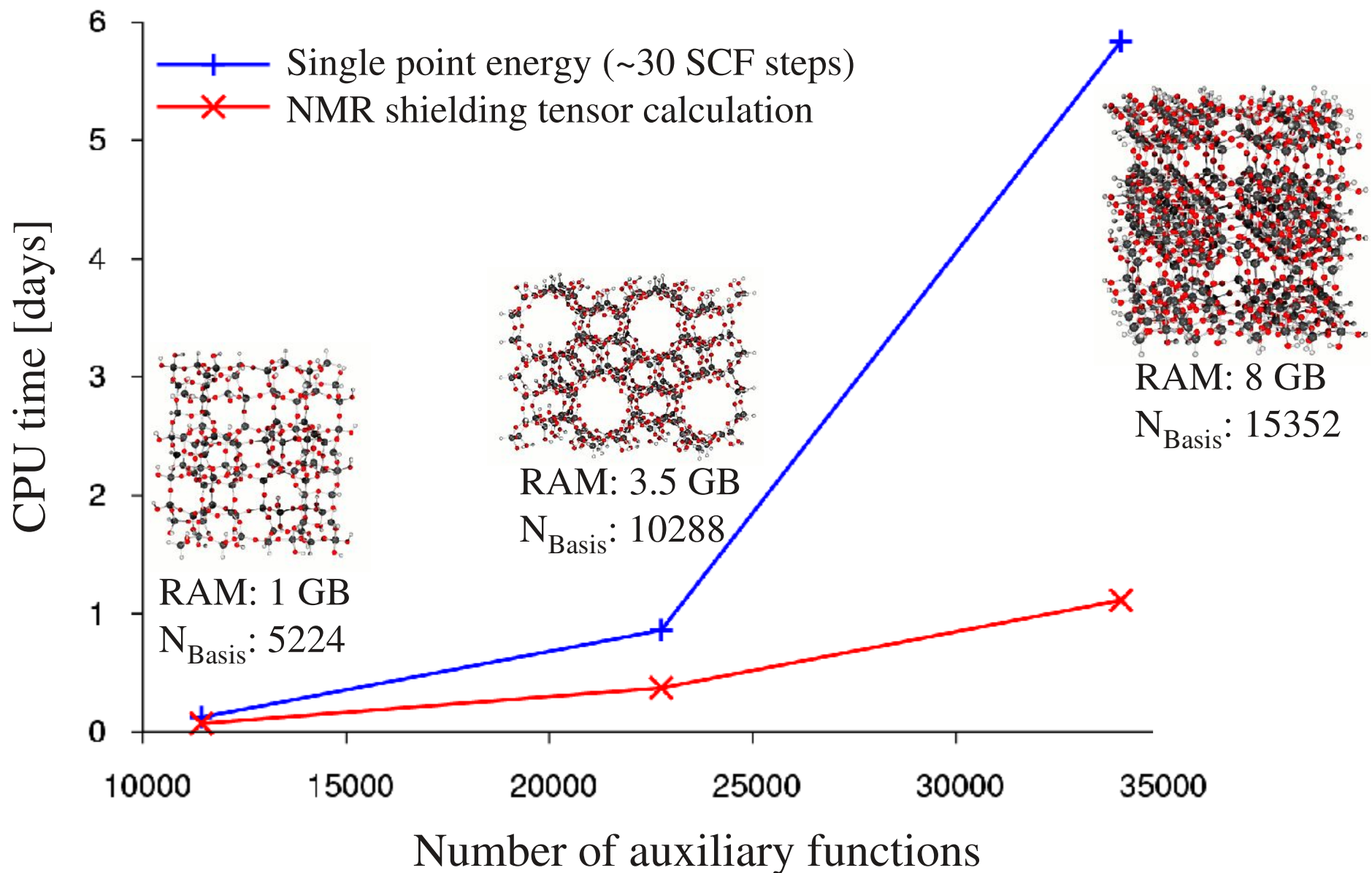
Oxygen



Comparison of Methodologies



GIAO-ADFT Performance on 10 x 2.4 GHz AMDs



GIAO-ADFT Magnetizability Tensor

deMon2k
density of Montréal

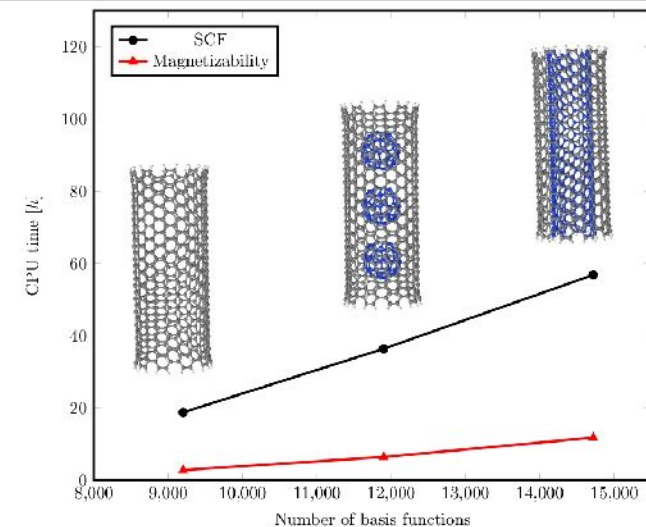
$$\xi_{xy} = -\lim_{\vec{H} \rightarrow 0} \frac{\partial^2 E}{\partial H_x \partial H_y} = \sum_{a,b} P_{ab} \left[H_{ab}^{(x,y)} + \sum_{\bar{k}} \langle \phi_a^* \phi_b \| \bar{k} \rangle^{(x,y)} (x_{\bar{k}} + z_{\bar{k}}) \right] + \\ \sum_{a,b} P_{ab}^{(x)} K_{ab}^{(y)} - \sum_{a,b} S_{ab}^{(x,y)} W_{ab} - \sum_{a,b} S_{ab}^{(x)} W_{ab}^{(y)}$$

Comparison of Methodologies [JT⁻²]

Molecule	HF ^a	CCSD ^a	CCSD(T) ^a	CCSD(T) ^{a,b}	VWN ^c	PW91 ^c	Expt.
CH ₄	-313	-316	-317	-316	-329	-317	-310 ^d
NH ₃	-287	-289	-290	-290	-298	-291	-290 ± 30 ^e
CH ₃ F	-318	-317	-316	-315	-316	-311	-315 ± 13 ^e
C ₂ H ₄	-354	-347	-346	-345	-330	-330	-334 ± 13 ^e
CH ₂ CCH ₂	-478	-481	-480	-478	-461	-453	-449 ± 13 ^e

^aFrom O.B. Lutæs, A.M. Taele, T. Helgaker, D.J. Tozer, K. Ruud, J.Gauss, *J. Chem. Phys.* **131**, 144104 (2009); ^baug-cc-pCV[TQ]Z basis set was used; ^cADFT-GIAO with aug-cc-pCVQZ/GEN-A2;

^dExp. data from J.G. Oldenziel, N.J. Trappeniers, *Physica A* **82**, 581 (1976); ^eExp. data (scaled by 1.07) from C. Barter, R.G. Meisenheimer, D.P. Stevenson, *J. Phys. Chem.* **64**, 1312 (1960).



B. Zuniga-Gutierrez, G. Geudtner, A.M. Köster, *J. Chem. Phys.* **137**, 094113 (2012)

GIAO-ADFT Rotational g-Tensor

Spin-Rotation Tensor:

$$g_{xy} = - \lim_{\vec{J} \rightarrow 0, \vec{\mathcal{H}} \rightarrow 0} \frac{\partial^2 E(\vec{J}, \vec{\mathcal{H}})}{\partial J_x \partial \mathcal{H}_y}$$

GIAO:

$$\begin{aligned}\varphi_a(\vec{r}, \vec{\mathcal{H}}) &= a(\vec{r}) e^{-i(\vec{\chi}_a^{\mathcal{H}} + \vec{\chi}_a^J) \cdot \vec{r}} \\ \vec{\chi}_a^{\mathcal{H}} &= \frac{1}{2} \vec{\mathcal{H}} \times (\vec{A} - \vec{G}) \\ \vec{\chi}_a^J &= - (I_{nuc}^{-1} \cdot \vec{J}) \times (\vec{A} - \vec{R}_{com})\end{aligned}$$

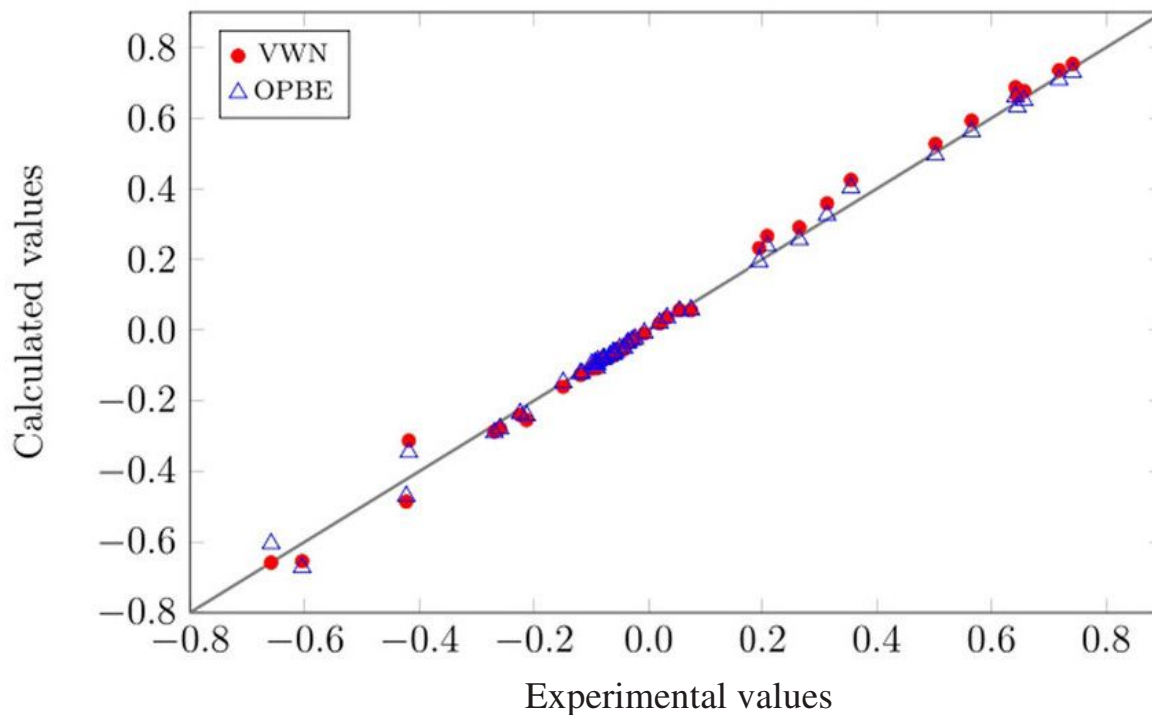


Figure 1. Comparison of the calculated ADFT-GIAO VWN and OPBE rotational **g** tensor diagonal elements with experimental data. The data are taken from Table 2

GIAO Integrals

Because of missing response in GIAO-ADFT molecular integral calculation becomes the computational bottleneck.

GIAO Overlap (Semi-Classical Perturbation Theory):

$$\begin{aligned} S_{ab} &= \lim_{\vec{H} \rightarrow \vec{0}} \langle \Phi_a | \Phi_b \rangle = \lim_{\vec{H} \rightarrow \vec{0}} \int a(\vec{r}) b(\vec{r}) e^{\frac{i}{2} \vec{H} \times (\vec{A} - \vec{B}) \cdot \vec{r}} d\vec{r} \\ &\simeq \int a(\vec{r}) b(\vec{r}) d\vec{r} + \lim_{\vec{H} \rightarrow \vec{0}} \frac{i}{2} \vec{H} \times (\vec{A} - \vec{B}) \int a(\vec{r}) \vec{r} b(\vec{r}) d\vec{r} = \langle a | b \rangle \end{aligned}$$

GIAO Overlap Derivative:

$$\begin{aligned} S_{ab}^{(x)} &\equiv \frac{\partial S_{ab}}{\partial H_x} = \lim_{\vec{H} \rightarrow \vec{0}} \langle \Phi_a^{(x)} | \Phi_b \rangle + \lim_{\vec{H} \rightarrow \vec{0}} \langle \Phi_a | \Phi_b^{(x)} \rangle \\ &= (A_y - B_y) \langle a | z | b \rangle - (A_z - B_z) \langle a | y | b \rangle \end{aligned}$$

GIAO-RI-DFT and GIAO-ADFT Shielding Tensor

$$\sigma_{xy}(C) = \lim_{\vec{H} \rightarrow \vec{0}, \vec{M}_C \rightarrow \vec{0}} \frac{\partial^2 E}{\partial H_x \partial M_{Cy}} = \sum_{a,b} P_{ab} H_{ab}^{(x,y)}(C) + \sum_{a,b} P_{ab}^{(x)} H_{ab}^{(y)}(C)$$

New GIAO Integral Recurrence Relation (like for ERIs):

Instead of independent P_{ab} and $H_{ab}^{(x,y)}(C)$ building, build directly the expectation value $\sigma_{xy}^D(C) = \sum_{a,b} P_{ab} H_{ab}^{(x,y)}(C)$!

Diamagnetic shielding operator:

$$\hat{\theta}_{xy}^D(C) = \frac{(x - C_x) y - \delta_{xy}(\mathbf{r} - \mathbf{C}) \mathbf{r}}{|\mathbf{r} - \mathbf{C}|^3}$$

Diamagnetic GIAO shielding tensor:

$$\sigma_{xy}^D(C) = -\frac{1}{2} \sum_{a,b} P_{ab} \langle a | \hat{\theta}_{xy}^D(C) | b \rangle$$

Diamagnetic Shielding Tensor Integrals

Definition of tensorial integral sums:

$$\sigma_{xy}^D(C) = -\frac{1}{2} t_{xy}^D(C) , \quad \sigma_{xx}^D(C) = \frac{1}{2} (t_{yy}^D(C) + t_{zz}^D(C))$$

$$t_{xy}^D(C) = \sum_{a,b} P_{ab} \left| ab \left| \frac{(x-C_x) y}{|\mathbf{r}-\mathbf{C}|^3} \right. \right|$$

Operator expansion:

$$\frac{(x-C_x) y}{|\mathbf{r}-\mathbf{C}|^3} = y \frac{\partial}{\partial C_x} \frac{1}{|\mathbf{r}-\mathbf{C}|^3} = y \hat{\mathcal{A}}_C(1_x) = (y - A_y) \hat{\mathcal{A}}_C(1_x) + A_y \hat{\mathcal{A}}_C(1_x)$$

Integral sum expansion:

$$\begin{aligned} t_{xy}^D(C) &= \sum_{a,b} P_{ab} \langle (a+1_y)b | \hat{\mathcal{A}}_C(1_x) \rangle + A_y \sum_{a,b} P_{ab} \langle ab | \hat{\mathcal{A}}_C(1_x) \rangle \\ &= \sum_{a,b} P_{ab} \langle ab | \hat{\mathcal{A}}_C(1_x) \rangle^{(y)} + A_y \sum_{a,b} P_{ab} \langle ab | \hat{\mathcal{A}}_C(1_x) \rangle \\ &= s_{xy}^D(C) + A_y s_x^D(C) \end{aligned}$$

Diamagnetic Shielding Tensor Integrals

New integral sums with respect to JCP **118**, 9943, 2003:

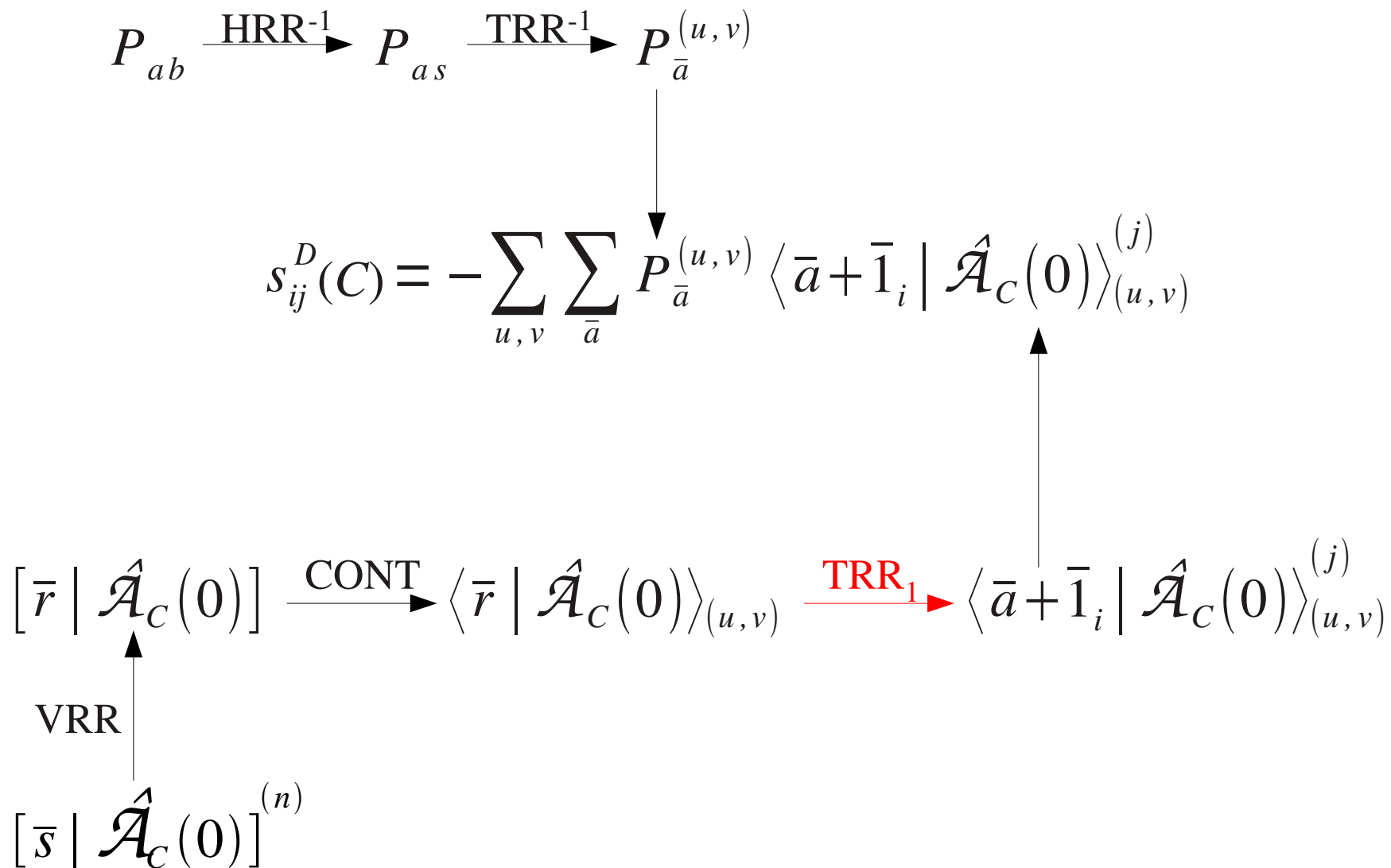
$$s_{xy}^D(C) \equiv \sum_{a,b} P_{ab} \langle ab | \hat{\mathcal{A}}_C(1_x) \rangle^{(y)} = - \sum_{u,v} \sum_{\bar{a}} P_{\bar{a}}^{(u,v)} \langle \bar{a} + \bar{1}_x | \hat{\mathcal{A}}_C(0) \rangle_{(u,v)}^{(y)}$$

New one-step transformation recurrence relation (TRR₁):

$$\begin{aligned} \langle \bar{a} + \bar{1}_i | \hat{\mathcal{A}}_C(0) \rangle_{(u,v)}^{(j)} &= (B_j - A_j) \langle \bar{a} + \bar{1}_i | \hat{\mathcal{A}}_C(0) \rangle_{(u+1,v+1)} + \\ &\quad \frac{1}{2} \langle \bar{a} + \bar{1}_i + \bar{1}_j | \hat{\mathcal{A}}_C(0) \rangle_{(u,v+1)} + \\ &\quad N_j(\bar{a}) \langle \bar{a} + \bar{1}_i - \bar{1}_j | \hat{\mathcal{A}}_C(0) \rangle_{(u,v)} \end{aligned}$$

Diamagnetic Shielding Tensor Integrals

Path diagram:



GIAO-RI-DFT and GIAO-ADFT Shielding Tensor

$$\sigma_{xy}(C) = \lim_{\vec{H} \rightarrow \vec{0}, \vec{M}_C \rightarrow \vec{0}} \frac{\partial^2 E}{\partial H_x \partial M_{Cy}} = \sum_{a,b} P_{ab} H_{ab}^{(x,y)}(C) + \sum_{a,b} P_{ab}^{(x)} H_{ab}^{(y)}(C)$$

$$P_{ab}^{(x)} = 2 \sum_o^{\text{occ}} \sum_u^{\text{uno}} \frac{K_{ou}^{(x)} - \epsilon_o S_{ou}^{(x)}}{\epsilon_o - \epsilon_u} c_{ao} c_{bu} + c_{au} c_{bo} - \frac{1}{2} \sum_{\mu,\nu}^{\text{occ}} P_{a\mu} S_{\mu\nu}^{(x)} P_{\nu b}$$

GIAO-RI-DFT Perturbed Kohn-Sham Matrix:

$$K_{ab}^{(x)} \equiv \frac{\partial K_{ab}}{\partial H_x} = H_{ab}^{(x)} + \sum_{\bar{k}} \langle \Phi_a^* \Phi_b \| \bar{k} \rangle^{(x)} x_{\bar{k}} + \langle \Phi_a^* | v_{xc}[\rho] | \Phi_b \rangle^{(x)}$$

GIAO-ADFT Perturbed Kohn-Sham Matrix:

$$K_{ab}^{(x)} \equiv \frac{\partial K_{ab}}{\partial H_x} = H_{ab}^{(x)} + \sum_{\bar{k}} \langle \Phi_a^* \Phi_b \| \bar{k} \rangle^{(x)} (x_{\bar{k}} + z_{\bar{k}}) ; \quad z_{\bar{k}} = \sum_{\bar{l}} \langle \bar{k} \| \bar{l} \rangle \langle \bar{l} | v_{xc}[\tilde{\rho}] \rangle$$

The Vanadium Atom Problem in DFT

TABLE III. Low-lying atomic states of the vanadium atom. The calculations were performed with the VWN-optimized basis set.

State	Configuration	$\Delta E_{\text{Cal.}}^{\text{VWN}}$ (eV)	$\Delta E_{\text{Cal.}}^{\text{PW86-P86}}$ (eV)	$\Delta E_{\text{Exp.}}$ (eV) ^a
V(⁴ F)	$s^2 d_{xy}^1 d_{xz}^1 d_{yz}^1$	0.00	0.00	0.00
V(⁶ D)	$s^1 d_{xz}^1 d_{yz}^1 d_{xy}^1 d_{x^2-y^2}^1$	0.91	0.51	0.25
V(⁶ S)	$d_{xy}^1 d_{yz}^1 d_{z^2}^1 d_{xz}^1 d_{x^2-y^2}^1$	1.02	1.58	2.47

^aC.E. Moore, *Natl. Bur. Stand.* **2**, 291 (1971)

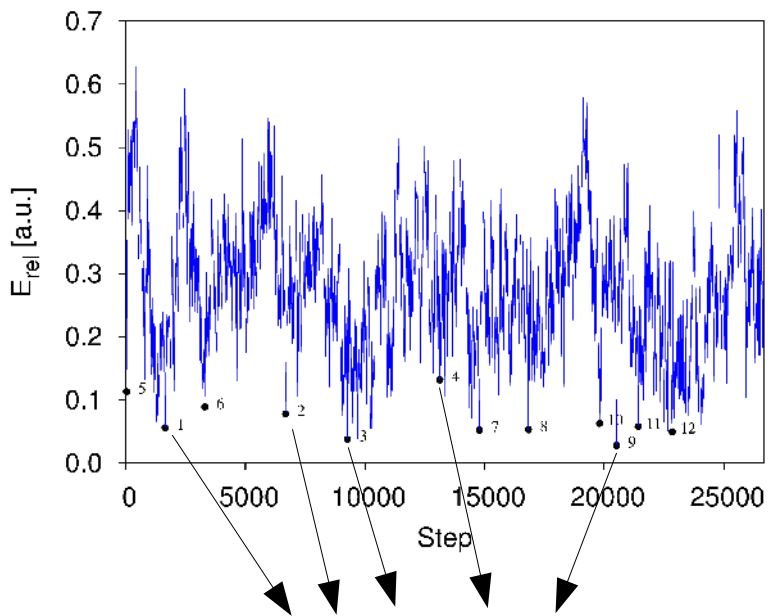
Vanadium Atom with GGA optimized Basis

State	Configuration	ΔE_{cal} [eV]	ΔE_{exp} [eV]
V(⁴ F)	$s^2 d_{xy} d_{xz} d_{yz}$	0.00	0.00
V(⁶ D)	$s d_{xy} d_{xz} d_{yz} d_{z^2}$	0.23	0.25
V(⁶ S)	$d_{xy} d_{xz} d_{yz} d_{z^2} d_{x^2-y^2}$	2.70	2.47
V ⁺ (~ ⁵ D)	$d_{xy} d_{xz} d_{yz} d_{x^2-y^2} (s d_{z^2})$	7.05	6.74
P. Calaminici, A.			01)
P. Calaminici, F.	V ⁺ (⁵ F)	7.23	7.03
V.M. Medel, A.C. Keber, V. Chauhan, P. Sen, A.M. Koster, P. Calaminici, S.N. Khanna, <i>J. Am. Chem. Soc.</i> 136 , 8229 (2014)			007)

Electronic Structure Methodology

- Exchange-correlation functional: PW86-P86
- Basis set: DZVP-GGA
- Auxiliary functions set: GEN-A2
- SCF Method: ROKS
- Adaptive grid accuracy: 10^{-5} a.u.
- Local optimization: Quasi-Newton restricted step method
- Frequency analysis: Finite differences of 0.001 a.u.
- Basis set for Ag: QECP with 19 valence electrons

“Global” Optimization Strategy



Start structures for local optimizations (~10)

Local optimization in Cartesian coordinates

Possible minimum structures (Selection by energy)

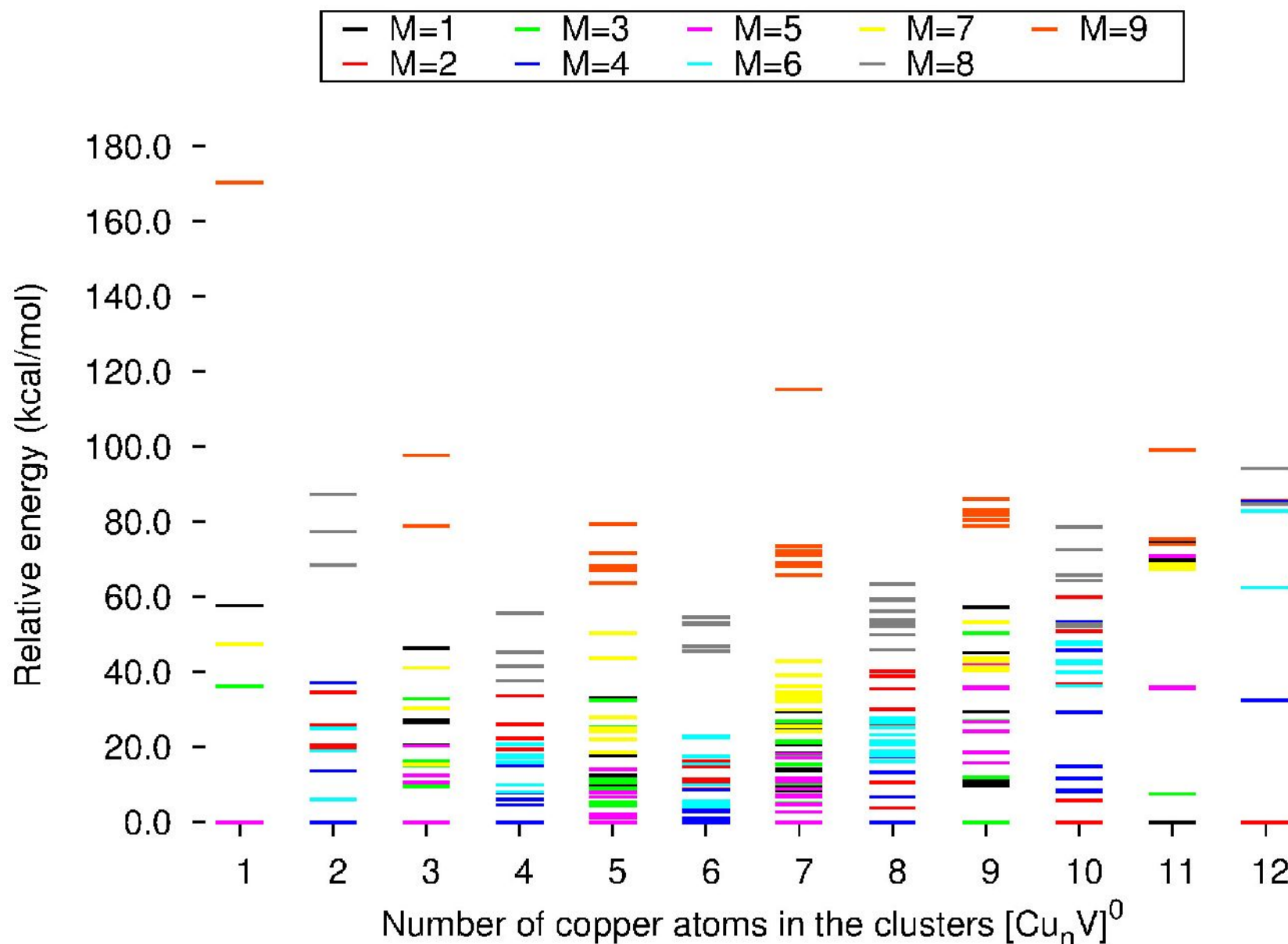
Characterization by frequency analysis

Minimum structures

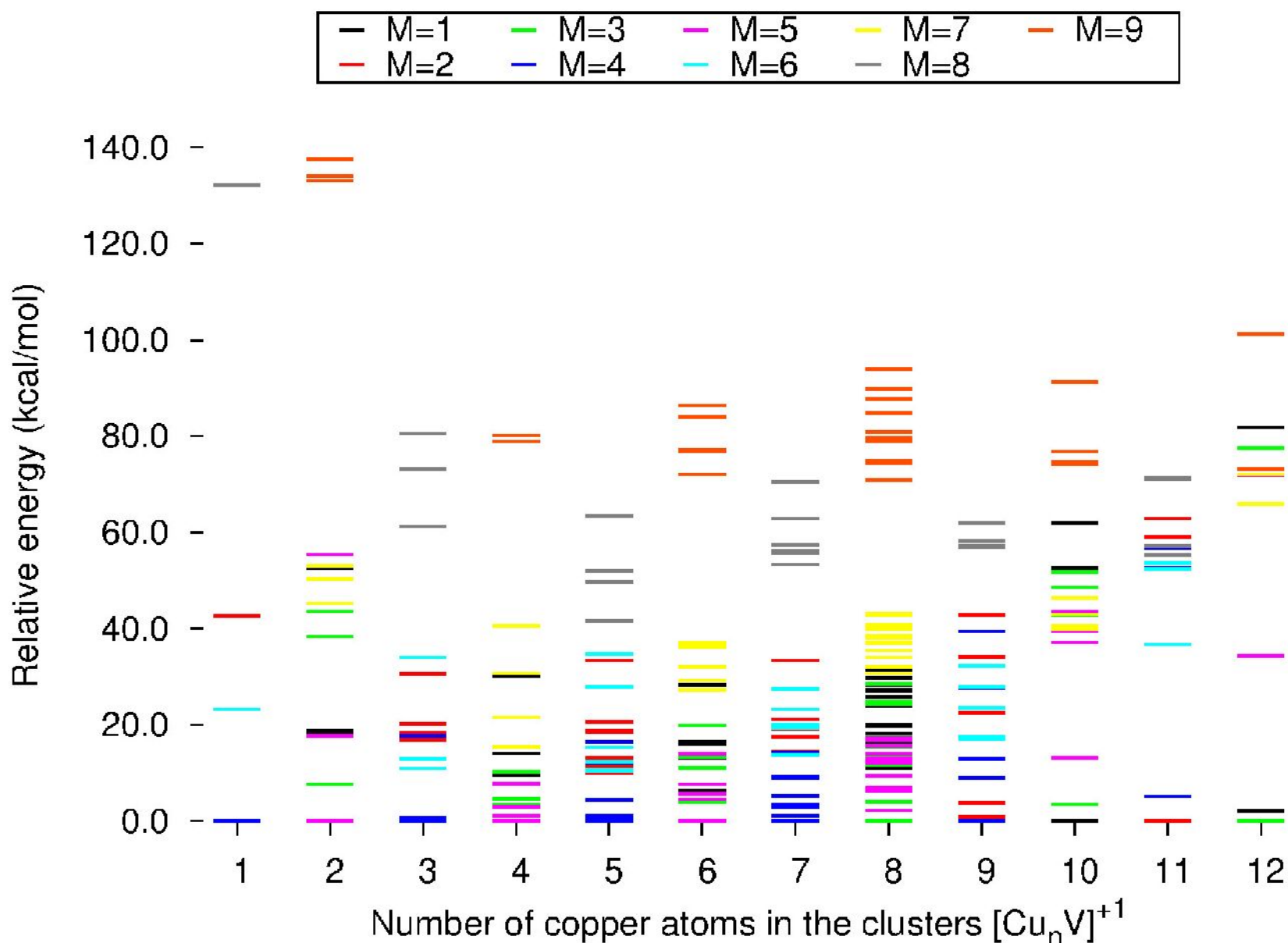
BOMD settings for each multiplicity:

- Step size: 2 fs
- Trajectories: 30 ps
- Temperature: 1500 K
- Thermostat: Nosé-Hoover (7 links)

“Global” Optimization Results

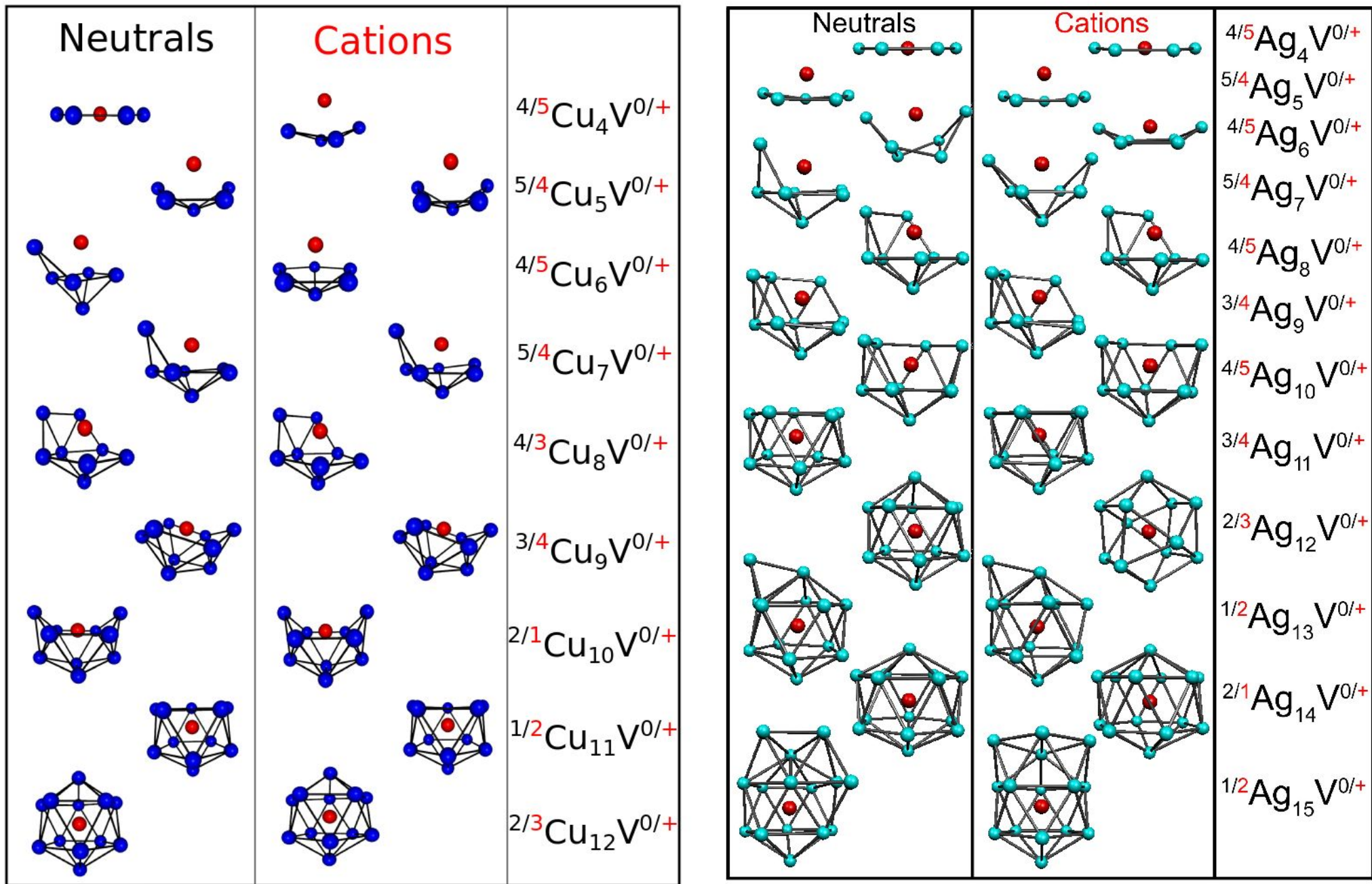


“Global” Optimization Results



$\text{Cu}_n\text{V}^{0/+}$ and $\text{Ag}_n\text{V}^{0/+}$ Ground State Structures

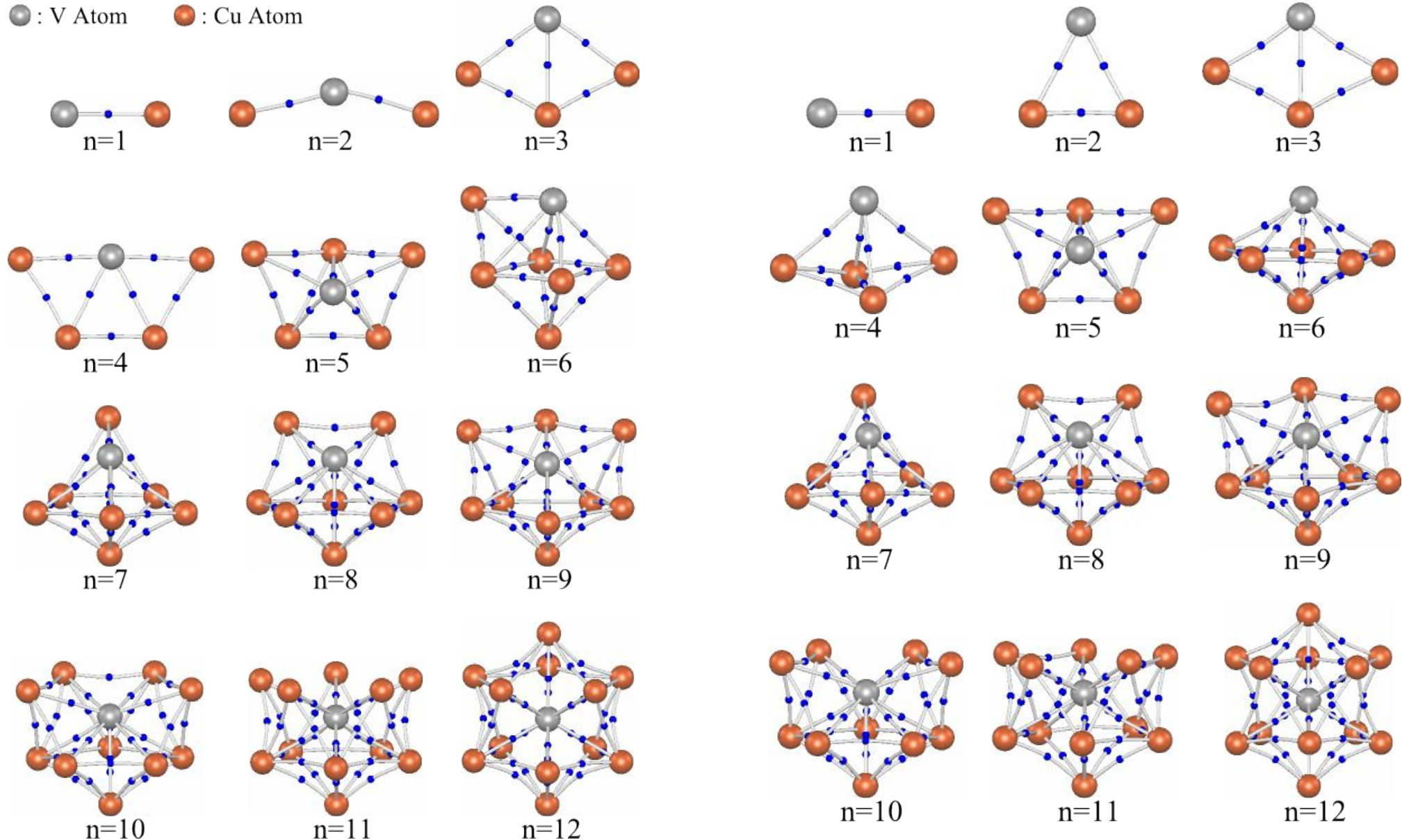
deMon2k
density of Montréal



➡ Structural similarity between $\text{Cu}_n\text{V}^{0/+}$ and $\text{Ag}_n\text{V}^{0/+}$ cluster (Exception n=12 cation)

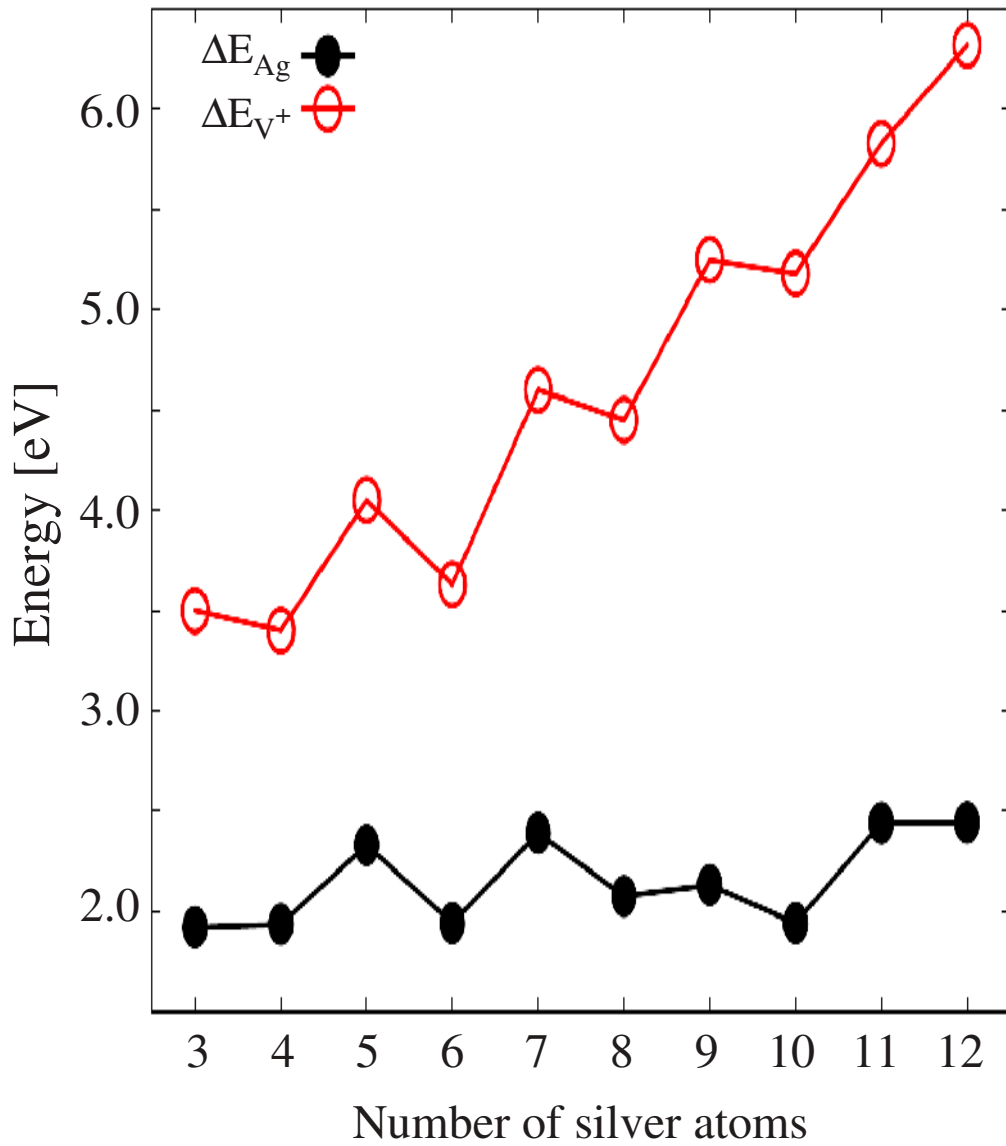
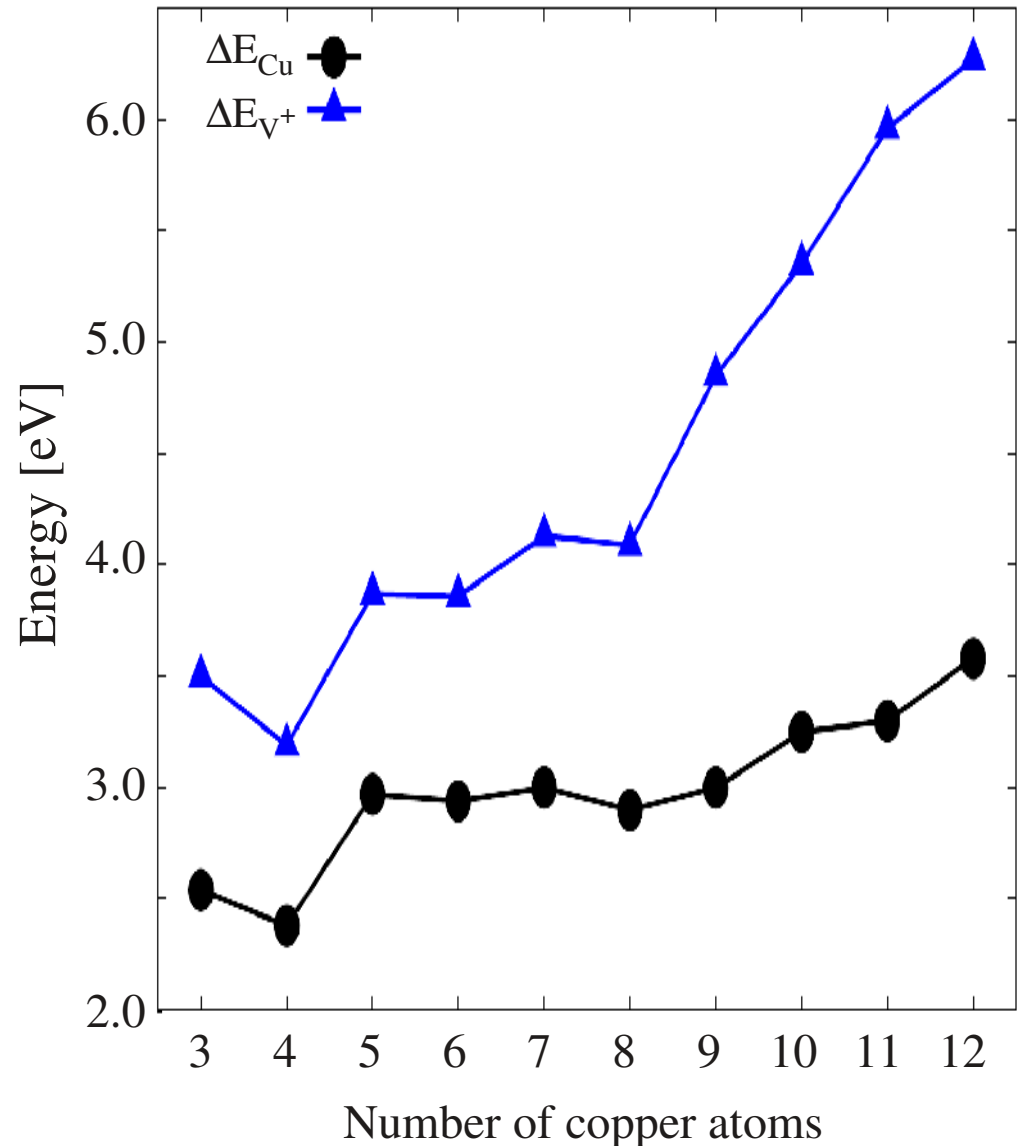
Molecular Graphs of $\text{Cu}_n\text{V}^{0/+}$ Clusters

● : V Atom ● : Cu Atom

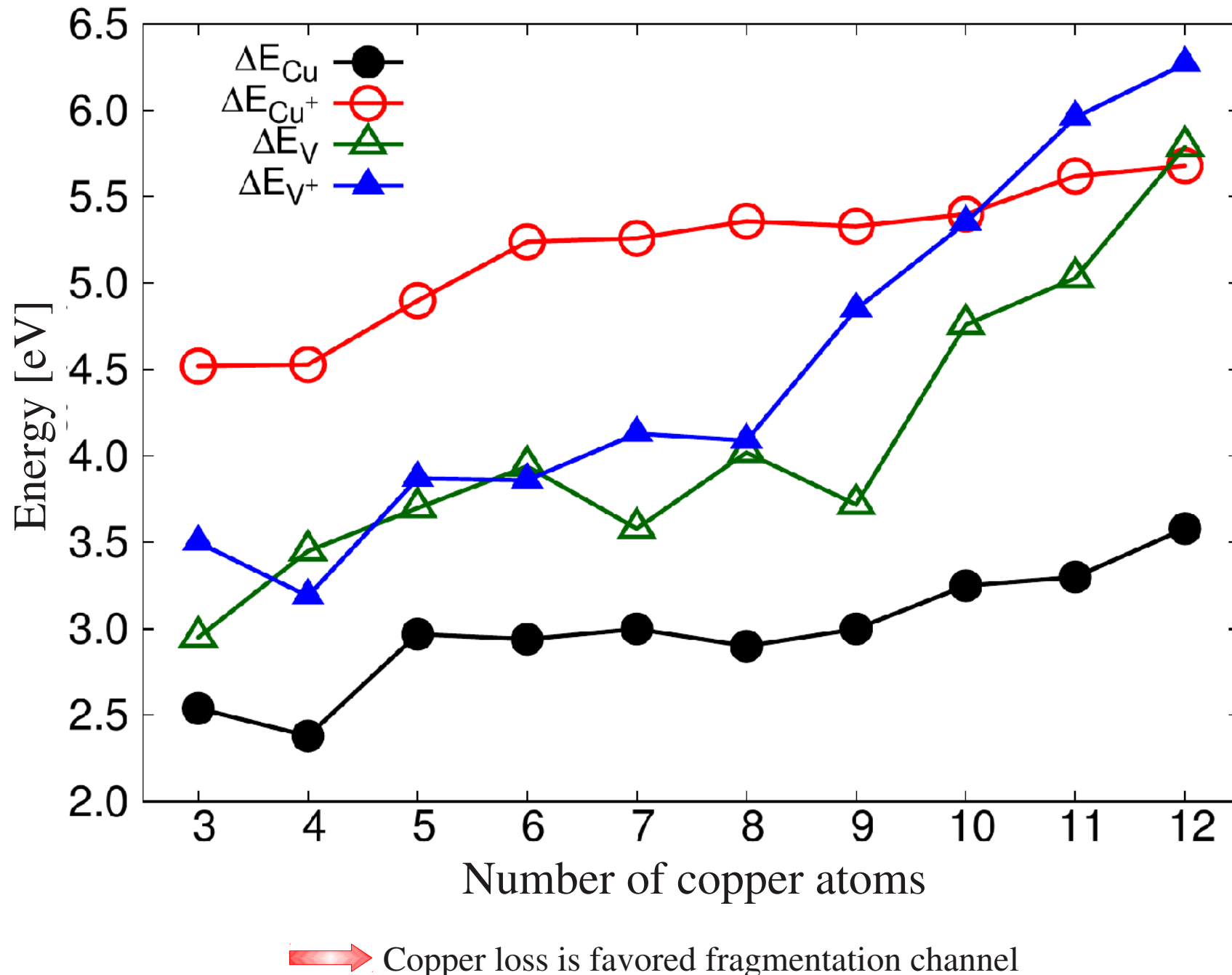


G. Geudtner, V.D. Dominguez-Soria, P. Calaminici, A.M. Köster, *Comp. Theor. Chem.* **1053**, 337 (2015)

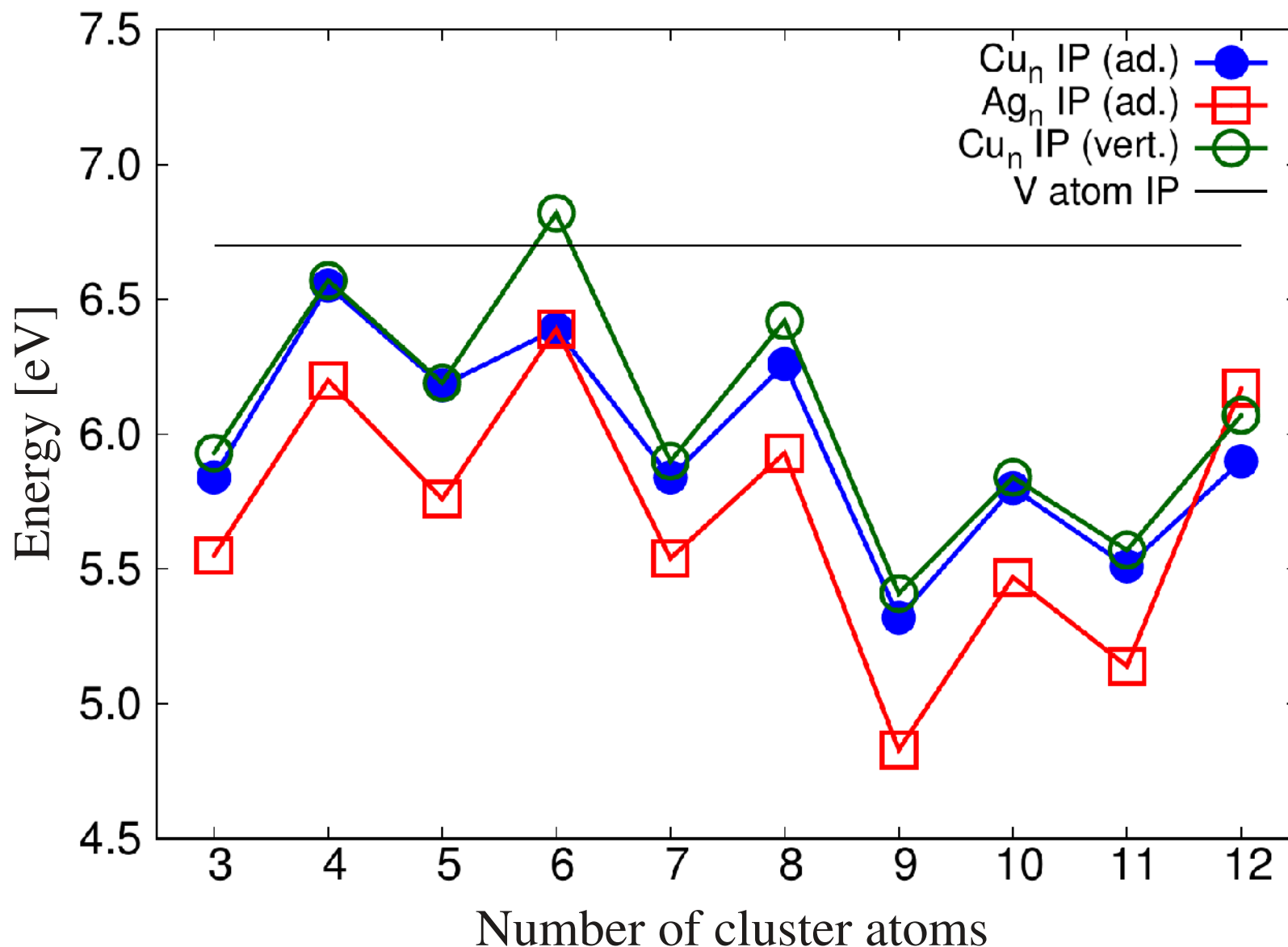
Cu_nV^+ and Ag_nV^+ Atom Loss Energies



Comparison of Cu_nV^+ Atom Loss Energies



Ionization Potentials



Atomic Valence Calculation

Bond order matrix:

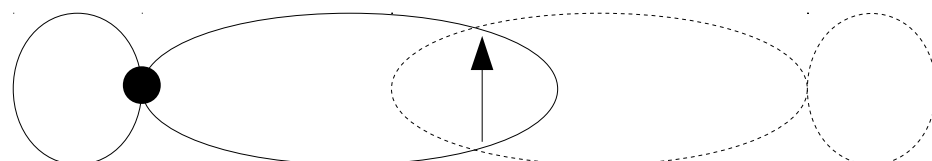
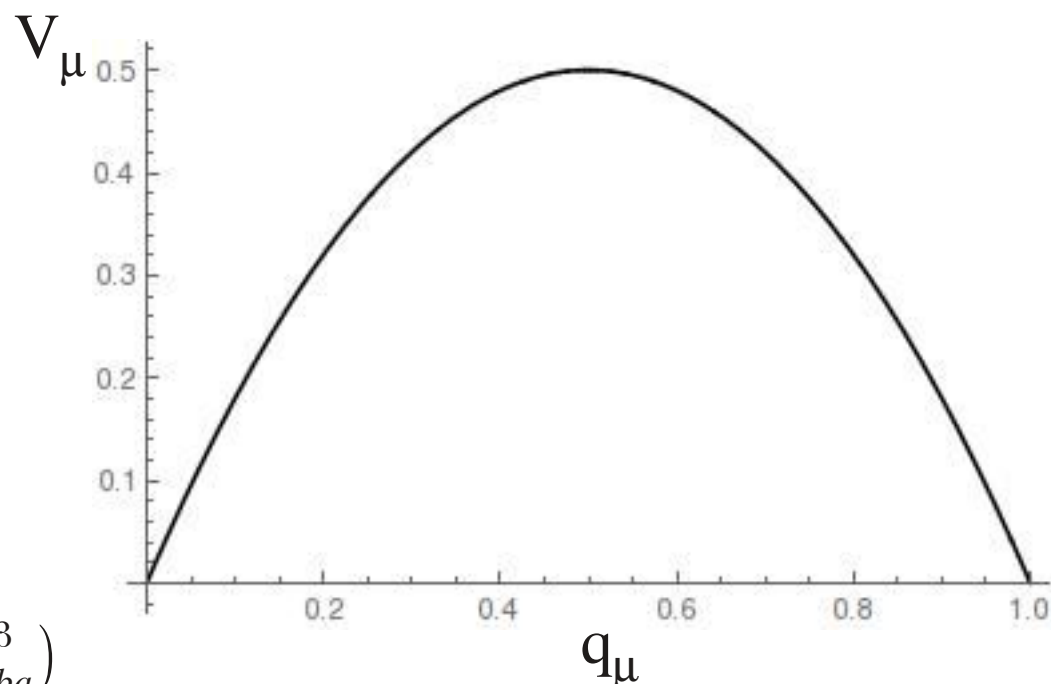
$$D_{\mu\nu} = \sum_{\sigma} P_{\mu\sigma} S_{\sigma\nu}$$

Closed-shell atomic valence:

$$V_A = \sum_a^A \sum_{B \neq A} \sum_b^B D_{ab} D_{ba}$$

Open-shell atomic valence:

$$V_A = 2 \sum_a^A \sum_{B \neq A} \sum_b^B (D_{ab}^\alpha D_{ba}^\alpha + D_{ab}^\beta D_{ba}^\beta)$$



M.S. Gopinathan, K. Jug, *Theor. Chim. Acta* **63**, 497 (1983)

I. Mayer, *Chem. Phys. Lett.* **97**, 270 (1983)

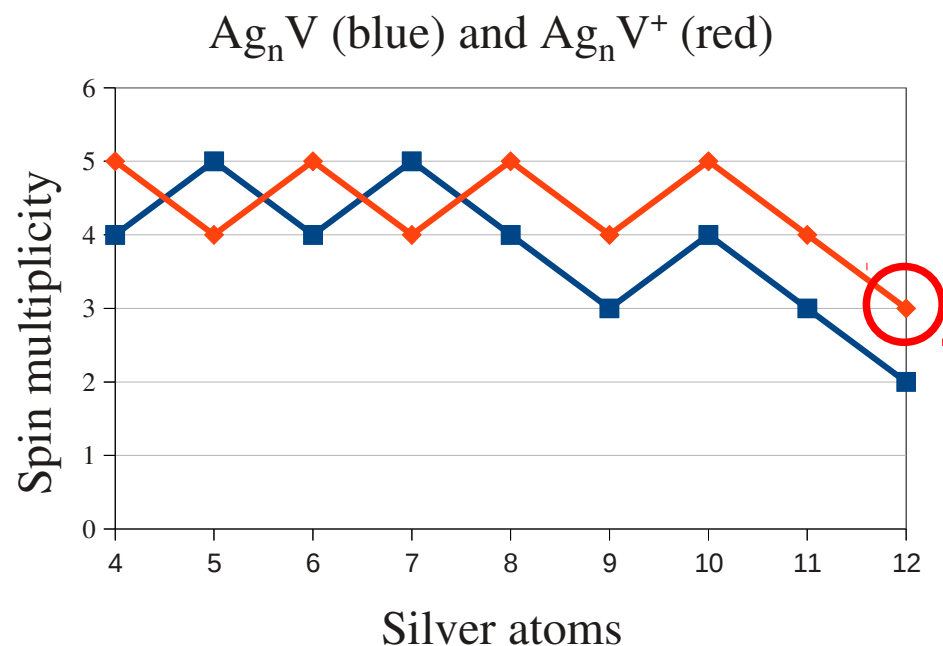
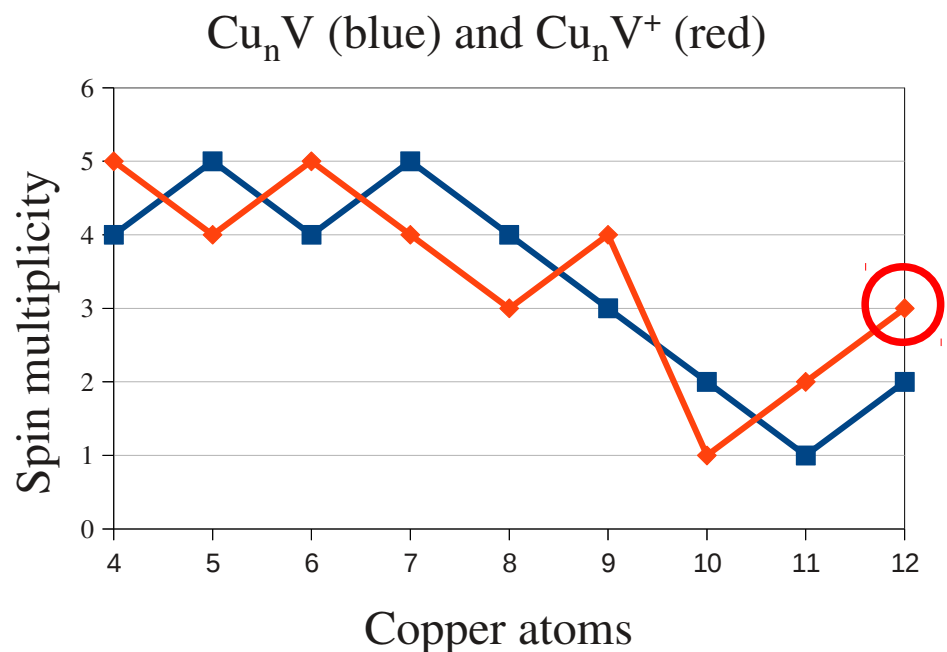
Vanadium Valence in $\text{Cu}_n\text{V}^{0/+}$ and $\text{Ag}_n\text{V}^{0/+}$

$\text{Cu}_n\text{V}^{0/+}$			$\text{Ag}_n\text{V}^{0/+}$		
n	Neutral	Cation	n	Neutral	Cation
4	2.7	2.4	4	2.4	2.1
5	2.7	2.9	5	2.6	2.7
6	3.0	3.0	6	3.0	2.6
7	3.5	3.6	7	3.1	3.1
8	4.2	4.3	8	3.5	3.3
9	4.6	4.7	9	3.9	3.7
10	4.9	5.2	10	4.1	3.9
11	4.9	5.3	11	4.4	4.1
12	5.0	5.8	12	4.8	3.8

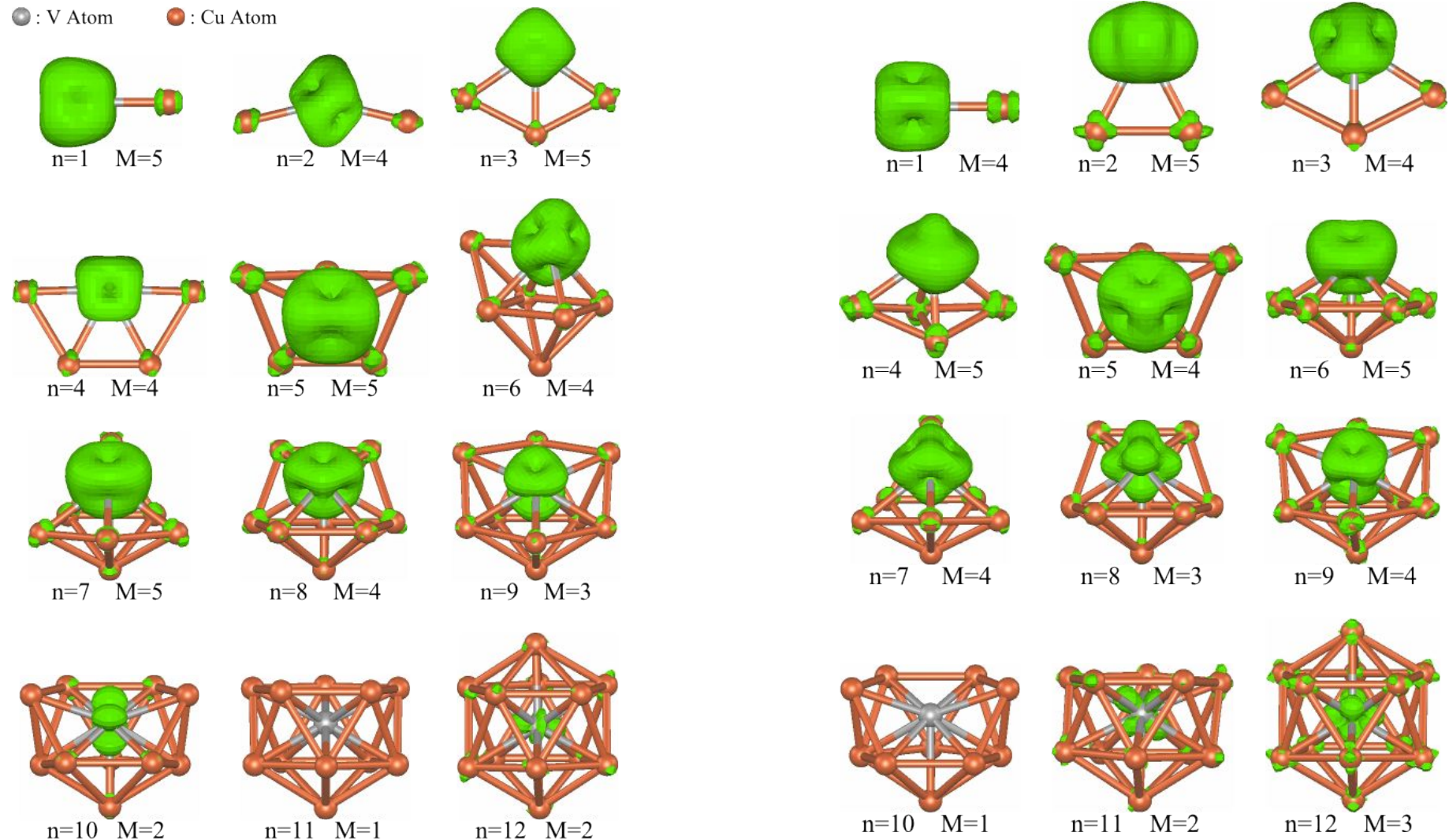
➡ Vanadium is stronger involved in cluster binding of $\text{Cu}_n\text{V}^{0/+}$ as of $\text{Ag}_n\text{V}^{0/+}$

$\text{Cu}_n\text{V}^{0/+}$ and $\text{Ag}_n\text{V}^{0/+}$ Ground State Multiplicities

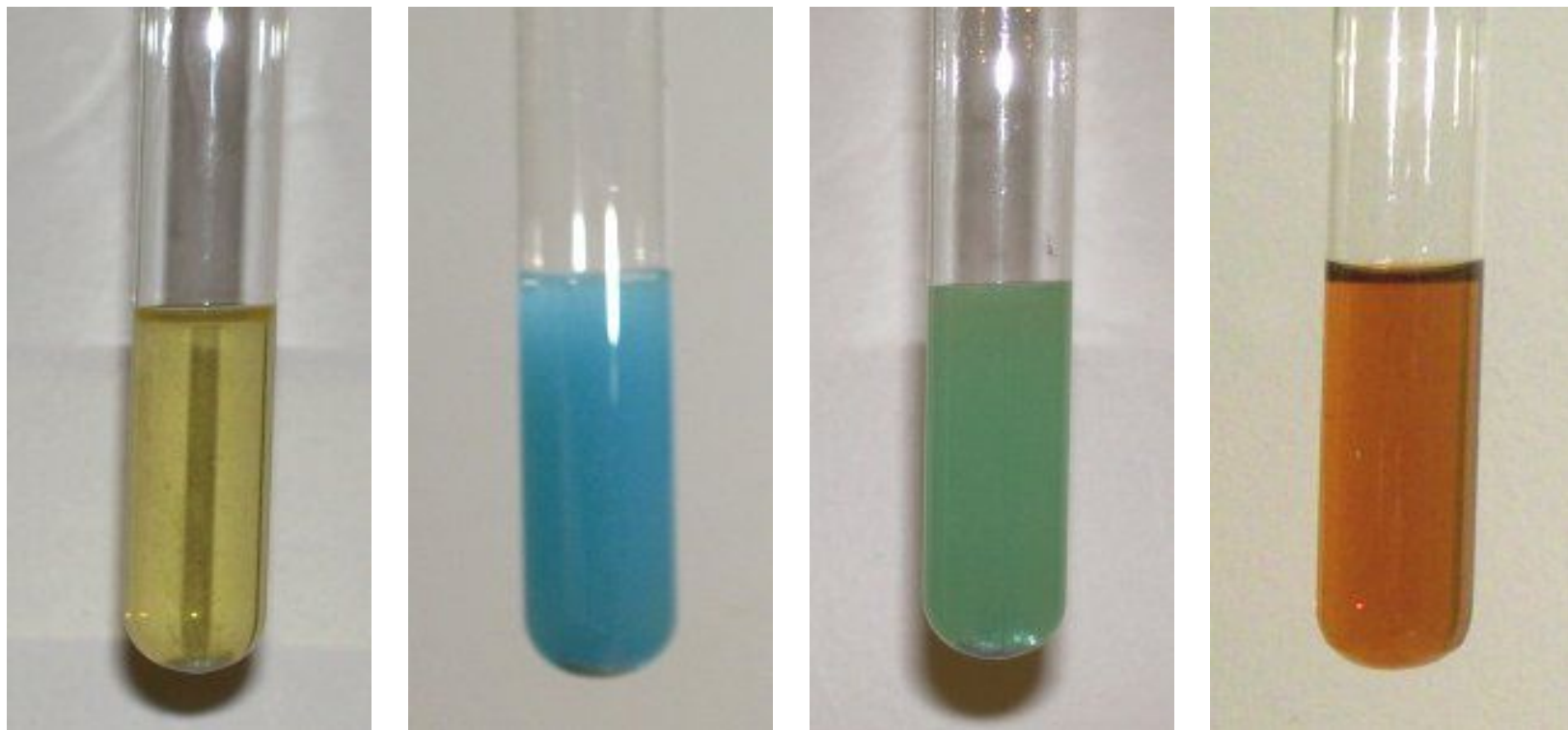
deMon2k
density of Montréal



Cu_nV and Cu_nV^+ Ground State Spin Densities



The Vanadium Chameleon



+5



+4



+3



+2

Vanadium oxidation states